Studying GPCR conformational dynamics by single molecule fluorescence

Robert Quast, Emmanuel Margeat

Studying GPCR conformational dynamics by single molecule fluorescence

Robert B. Quast and Emmanuel Margeat

CBS, CNRS, INSERM, Université de Montpellier, Montpellier, France

Corresponding Author

* Emmanuel Margeat: margeat@cbs.cnrs.fr

Abstract

Over the last decades, G protein coupled receptors (GPCRs) have experienced a tremendous amount of attention, which has led to a boost of structural and pharmacological insights on this large membrane protein superfamily involved in various essential physiological functions. Recently, evidence has emerged that, rather than being activated by ligands in an on/off manner switching from an inactive to an active state, GPCRs exhibit high structural flexibility in the absence and even in the presence of ligands. So far the physiological as well as pharmacological impact of this structural flexibility remains largely unexplored albeit its potential role in precisely fine-tuning receptor function and regulating the specificity of signal transduction into the cell. By complementing other biophysical approaches, single molecule fluorescence (SMF) offers the advantage of monitoring structural dynamics in biomolecules in real-time, with minimal structural invasiveness and in the context of complex biological environments. In this review a general introduction to GPCR structural dynamics is given followed by a presentation of SMF methods used to explore them. Particular attention is paid to single molecule Förster resonance energy transfer (smFRET), a key method to measure actual distance changes between two probes, and highlight conformational changes occurring at timescales relevant for protein conformational movements. The available literature reporting on GPCR structural dynamics by SMF is discussed with a focus on the newly gained biological insights on receptor activation and signaling, in particular for the β2 adrenergic and the metabotropic glutamate receptors.

Introduction

With some 800 members, G protein coupled receptors (GPCRs) constitute the largest membrane protein superfamily encoded in the human genome (Lagerström and Schiöth, 2008). Spanning the cellular plasma membrane, GPCRs translate extracellular signals, mediated by e.g. photons, ions, small organic molecules, lipids, sugars, peptides and proteins, into the interior of the cell, where downstream effector proteins are recruited and activated. The resultant initiation of precisely defined but highly complex signaling cascades leads to diverse cellular responses, regulating some of the most essential physiological functions involved in for instance the endocrine, cardiovascular, neurological and reproductive systems but also vision, taste and smell. Hence, a detailed understanding of the molecular mechanisms governing GPCR activation and signal transduction is of great interest for the development of novel drugs, fragrances and food supplements.

In the intrinsically allosteric mechanism of GPCR activation, an external stimulus leads to conformational rearrangements that are translated through the structural core, formed by seven mostly α-helical transmembrane spanning segments, and pass the signal on to transducers such as G proteins, GPCR kinases and arrestins. This activation model stems from decades of biochemical experiments, as well as crystallography and cryo-EM studies, capable of capturing snapshots of receptor conformations at high resolution Figure 1. Crystallography combined with x-ray diffraction can provide indirect information on dynamic features through calculation of B-factors while cryo-EM bears the potential to capture receptors in multiple conformations. Through the stabilization of distinct conformations by protein engineering, ligands, detergents, antibodies, nanobodies and transducers more than

250 structures of GPCRs have been solved and deposited up to date, comprising conformations that can be assigned to inactive, active but also intermediate states (for some recent reviews of GPCR structure and dynamics readers are referred to (Erlandson et al., 2018; Latorraca et al., 2017; Thal et al., 2018; Weis and Kobilka, 2018)). Although the structural features observed for the N-terminal part and the ligand binding pocket are evidently receptor-specific, receptor activation appears to involve a conserved, major reorganization of the cytoplasmic side (Figure 1). Upon activation, a large (10-15Å) outward movement of transmembrane helix 6 (TM6) is combined with rearrangements of other helices (TM5 and TM7), exposing an intracellular pocket that can effectively engage G proteins and other effectors.

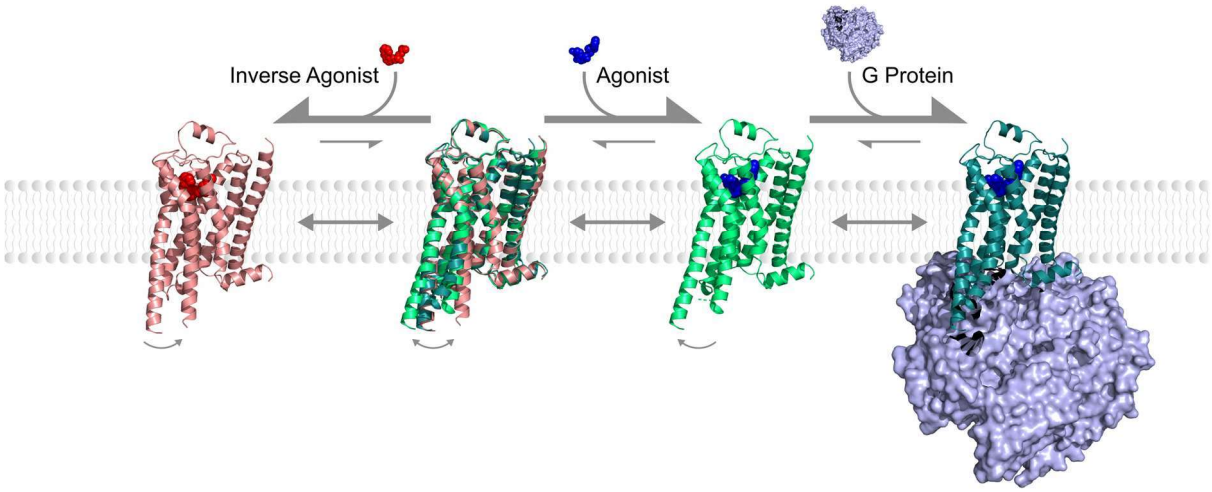

Figure 1: Structural flexibility of GPCRs exemplified on β2AR. In the absence of ligand, the receptor samples multiple conformations. Ligand binding shifts the equilibrium of the conformational ensemble in accordance with its pharmacological effect. Inverse agonists (red) lead to decreased population of active states (salmon, 2RH1) whereas agonists (blue) shift the equilibrium towards active states (green, 3P0G). The fully activated conformation (turquoise, 3SN6) is stabilized by additional binding of transducers, here the G protein (cyan).

However, these structures often represent states of local energy minima that are favored by the individually applied experimental conditions. In the meantime great efforts in membrane protein purification and engineering accompanied by significant technological advances, have enabled sophisticated biophysical studies, to demonstrate that activation of GPCRs is highly dynamic and seems not to be sufficiently explained by a simple on/off transition from a static inactive to a distinct active states (Figure 1).

In particular nuclear magnetic resonance (NMR)(Casiraghi et al., 2019), double electron-electron resonance (DEER) (Wingler et al., 2019) fluorescence spectroscopy together and molecular dynamics simulations (Latorraca et al., 2017) have provided evidence for the presence of multiple conformational states that are visited during GPCR activation, with a state being defined as an ensemble of multiple

rapidly interchanging single conformations, which coexist as intermediates in equilibrium with active and inactive states (Figure 1). Generally, individual conformational states can be described to represent local energy minima that result from the ensemble of atomic interactions within a molecular structure. Experimentally, these states are assigned to individual protein conformations, which may either be stable enough or populated with sufficient frequency over a given period of time to be detected by a certain method. Thus, a careful consideration of experimental methods is of great importance and complementary approaches are often necessary to elucidate the intrinsically dynamic properties of conformational states. In such a dynamic scenario, the effect of ligands on receptor conformation can be exerted by i) altering the time period a receptor populates a certain state (ie changing the height of the activation barrier between states), ii) modulating the relative population of the various states (ie changing the relative free energy of the states), and iii) enabling the adoption of a new conformational state that was not visited in its absence (ie lowering the free energy of this additional state and/or the activation barrier to reach it). In a similar way to orthosteric ligands, interaction with transducers and other receptor molecules, the local membrane environment, the pH and posttranslational modifications can function as external “perturbations” to allosterically modulate intrinsic receptor dynamics and fine-tune the conformational equilibrium (Thal et al., 2018). Indeed, for several GPCRs allosteric interactions seem to be indispensible for full activation, suggesting a rather loose link of agonist induced conformational changes in the ligand binding pocket and those in the intracellular TMD regions that account for interactions with the transducers.

Ligand efficacy is described as the measure of the extent to which a certain ligand is capable of inducing a physiological response. Thus, ligands have been classified in

groups according to their effects on GPCR signal transduction relative to the unliganded basal state, comprising activating full and partial agonists, inactivating inverse agonists as well as neutral antagonists that compete with the aforementioned for occupying the orthosteric site (Wacker et al., 2017). Interestingly, some ligands activate G proteins but also recruit arrestins while others are distinctively biased towards one pathway or the other, a phenomenon known as ligand-biaised agonism (Smith et al., 2018). The characterization of short-lived conformational states that result from the intrinsic structural flexibility of GPCRs, that may be further influenced by allosteric mechanisms, could provide new insights into the molecular basis of this phenomenon. However, the characterization of these states remains experimentally challenging due to their instability. In this context, understanding the full pharmacological spectrum of these receptors requires methods that allow investigating their dynamics, while revealing instable, poorly populated states.

In the following we will describe the basis of protein structural dynamics and the methods that allow exploring them. Subsequently, we will focus on single molecule fluorescence (SMF) methodologies to explore these dynamic properties, pointing out their advantages and limitations. This will be followed by a review on the biological insights that have been permitted by applying SMF to study the structural dynamics of GPCRs. Finally, we will attempt to evaluate the impact that SMF will have on our understanding of structural dynamics in the field of GPCR research and how it may lead to new strategies of drug discovery.

Single molecule methodologies for exploring structural dynamics

Timescales of protein dynamics

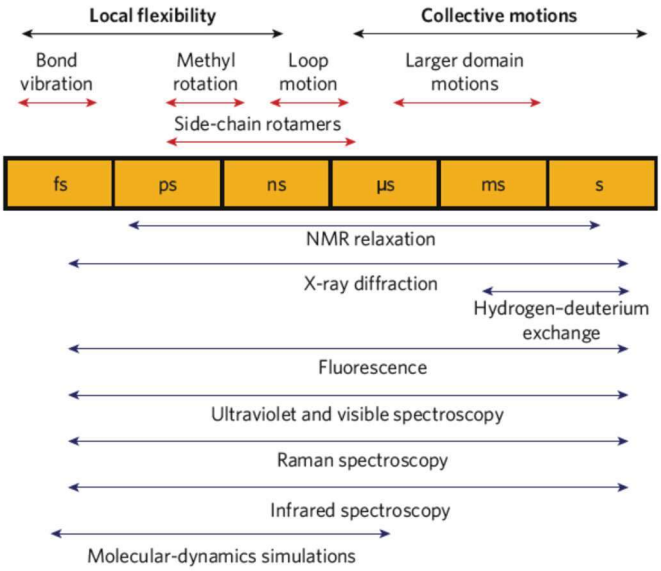

Figure 2: Timescale of dynamic processes in proteins and the experimental methods that allow detection of these fluctuations for each timescale. Reprinted from (Henzler-Wildman and Kern 2007).

Proteins used to be considered as static entities, in part because of the view inherently given by the only technique then available to study their structure, X-ray crystallography. However, a wide range of biophysical and computational techniques nowadays allow to characterize the multiple conformations that interconvert during protein function, resulting from the fluctuations of complex networks of non-covalent bonds (Figure 2) (Henzler-Wildman and Kern, 2007). The timescales of these fluctuations can now be measured as well, and energetic landscapes of protein conformational dynamics can be constructed.

Local motions such as residue side-chain rotations or movements of small loops typically take place in the nanosecond to microsecond time-scale. Larger-scale movements typically occur between a discrete number of states, energetically separated by a barrier of several kT, and thus happen at a slower timescale, ie µs-

ms and slower. All these movements can be measured by a number of spectroscopic methods, including NMR, fluorescence, UV-visible or IR spectroscopies (Henzler-Wildman and Kern, 2007). Moreover, sub-millisecond movements are accessible to all-atoms computational simulations, while slower conformational changes have to be sampled by coarse-grained simulations (Alhadeff et al., 2018; Hollingsworth and Dror, 2018). Finally some conformational changes only happen after a chemical reaction, and therefore can take place at much slower timescales. These types of movements are typically observed in enzymes or molecular motors.

Observation of protein dynamics at the single molecule level

Simultaneously extracting structural and kinetic information from a biomolecular complex in motion is ideally performed by directly monitoring single molecules in real-time. Single molecule observation can indeed reveal the presence of molecular subpopulations, and provides the opportunity to directly follow complex reactions that cannot be or do not need to be synchronized (Mehta et al., 1999; Weiss, 1999). A set of different technologies allow for this observation including force-based methods (such as optical (Ashkin et al., 1987) and magnetic tweezers (Strick et al., 1996) or atomic force microscopy (Engel et al., 1999)), single ion-channel recordings (Sackmann and Sakmann, 1992), as well as various spectroscopy methods, mainly derived from molecular fluorescence (Soper et al., 1990). Force-based methods have been extensively used to characterize molecular motors, or to uncover the topology and energetic properties of proteins, for example during unfolding. However, the fact that they require the attachment of the protein-of-interest (POI) to micrometer-sized handles limits their use to study structural dynamics, as they may severely alter conversion rates and conformational freedom. Conversely, single

molecule fluorescence only requires the specific attachment of a fluorescent probe (since generally proteins are not fluorescent in the visible wavelengths that are required for single molecule observation). Fluorescent probes are excellent reporters of conformational changes that affect their direct molecular environment, as these fluctuations can influence their spectral properties, excited-state lifetime, or rotational freedom (see below). Furthermore, some single molecule fluorescence experiments do not require immobilization of the POI, and can be performed in living cells (Schmidt et al., 1996).

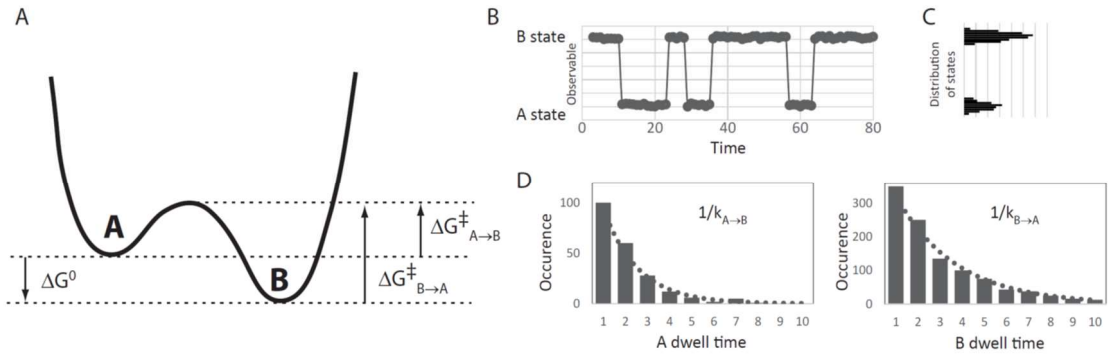

Figure 3: Extraction of structural dynamics information from single molecule fluorescence experiments. In an idealized model, two energetically separated states (A) are differentiated by plotting fluctuations of the observable over time (B) or the plot of the distribution of the states (C). Analysis of the dwell times the observable spends in each of the states allows for extraction of transition rates between the two states (D).

Ideally, a single molecule experiment should yield an observable that reports on the conformational movement under study, at a time resolution higher than the characteristic time of this movement. To illustrate this concept, we will consider a very simple system, such as a protein in equilibrium between two states (A and B, see Figure 3A). These states are characterized by a free energy difference ΔG^0, which will define their relative population at equilibrium. The transition probability

between these states, and thus the timescale of this transition, is related to the height of the energy barrier between them, and thus the free energies of activation $\Delta G^{\ddagger}_{A\rightarrow B}$ and $\Delta G^{\ddagger}_{B\rightarrow A}$ (transition from state A to B and vice-versa, respectively). The ideal single molecule experiment will yield an observable for each state, and thus recording this signal for a molecule over an extended period of time will yield a time–trace such as Figure 3B, that reports directly on the transitions between the two states as a function of time. From this trace, the plot of the distribution of states (Figure 3C) will directly report on the occupancy of the two states at equilibrium, and thus the equilibrium constant K_{eq} and the free energy difference between the states ΔG^{0}, as follows:

$$K_{eq} = \frac{[B]}{[A]} = e^{\frac{-\Delta G^{\circ}}{RT}}$$

, where R is the ideal gas consant and T the temperature.

In addition, the distribution of the observed dwell time the molecules spent in each state will report on the transition probability from one state to the other. In the case of the 2-state model mentioned above, dwell time distributions of states A and B (Figure 3D) can be fitted with single exponential decay functions, reporting on the kinetic rate constants for transitions from A to B ($k_{A\rightarrow B}$) and B to A ($k_{B\rightarrow A}$), respectively. These rate constants are proportional to the free energies of activation, that can be recovered by performing this kinetic measurement at different temperatures (Arrhenius plot), since

$$k_{A\rightarrow B} = A.e^{\frac{-\Delta G^{\ddagger}_{A\rightarrow B}}{RT}}$$

, where A is a pre-exponential factor, constant for each reaction.

This type of dwell-time analysis can identify the presence of hidden states (for example having the same signature than state A or B in the single molecule

observable) that could be revealed for example due to the presence of a multiexponential decay in the dwell time analysis. More sophisticated analysis such as hidden Markov modeling can also be performed when multiple states are apparent, in order to extract the transition rates and the pathways between them (McKinney et al., 2006).

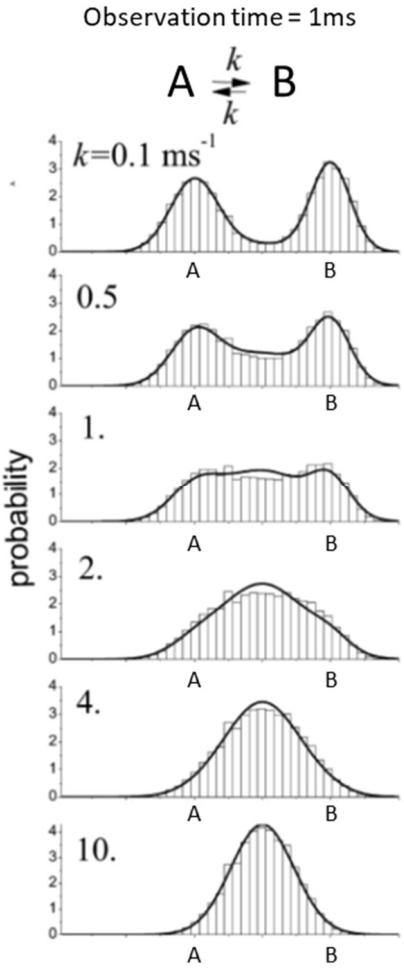

Figure 4: Relationship between timescale of conformational dynamics and observation time. When transition rates between states A and B are shorter than the observation time (<1ms), a clear differentiation is obtained between the two states when plotting the probability versus the observable. On the contrary, transition rates longer than the observation time result in a merge of the two peaks only providing an average value. (mofified from (Gopich and Szabo, 2010))

Unfortunately, molecular motions in proteins often occur at characteristic timescales that are in the order or faster than the time resolution of a single molecule fluorescence experiment. In such a case, the experimentally observed value will be related to the fraction of time the molecule spends in each state, time-averaged over the complete observation time. This is illustrated in Figure 4, illustrating the distribution of an experimental observable at a time resolution of 1ms, as a function of the transition rate constants between two states (A and B, for simplification the transition rate $k_{A\rightarrow B}$ and $k_{B\rightarrow A}$ are equal to k). If the transition rate is slower (k=0.1ms^{-1}) than the observation time (Figure 4, top), the two states are well defined, and their relative characteristics and relative population can be measured. However, for faster transitions, the two distributions start to merge, until they appear as a single distribution (Figure 4, bottom), in the case where the transition rate (k=10ms^{-1}) is ten times faster than the observation time. Fortunately, sophisticated data analysis methods have been developed to partially unveil the kinetic and structural parameters hidden in such distributions. In the case of single molecule fluorescence treated below, correlation, excited state lifetime distribution, and photon distribution analysis allow for such quantifications (Felekyan et al., 2013; Kalinin et al., 2010; Laurence et al., 2004; Torella et al., 2011).

Single molecule fluorescence

Fluorophores are small conjugated electronic systems that absorb radiation and, after relaxation, reemit a photon, typically at a longer wavelength. Several parameters characterize this phenomenon collectively named fluorescence, and all of them can be used as reporters of the local environment of the fluorophore (Lakowicz, 2006).

1 / The Stokes shift represents the difference between the positions of the band maxima of the absorption and emission spectra. For some environmentally sensitive dyes, a change in the exposure to solvent will influence the relaxation of this fluorophore. This will result in a change in the position of the emission maximum, which can be measured in a spectrally resolved experiment.

2/ The excited state lifetime represents the average time the fluorophore spends in the excited states, and is typically in the nanosecond timescale. It can be measured through a time-resolved experiment, and can report on short range interactions of the fluorophore with its environment, such as Förster energy transfer (see below).

3/ The rotational properties of the fluorophore can be measured as well, since its transition moment depends on its physical orientation. The excitation of a fluorophore is more efficient if its transition moment is parallel to the electric vector of the incident photon and the polarization of the emitted light also depends on the transition moment. Thus, measuring the polarization of the emitted light will report on how freely the fluorescent molecule moves during the time spent in the excited state.

4/ Finally, the quantum yield represents the efficiency of the fluorescence process, defined as the probability of a fluorophore to emit a photon after absorption of an incoming photon. Local environmental factors, such as steric constraints that will influence the structure of the chromophore, or the proximity of electron donor or acceptor groups, influence the emitted fluorescence intensity by quenching or enhancing the efficiency of this process.

The ability to detect and quantify the emission of single fluorophores using far-field microscopy at room temperature has been established in the mid-nineties (Nie et al., 1994; Schmidt et al., 1996). Besides detecting fluorescence intensities, the experimental determination of spectral properties for single fluorophores (Macklin et

al., 1996), excited state lifetimes (Macklin et al., 1996; Muller et al., 1996), polarization (Ha et al., 1998), as well energy transfer between two fluorophores (FRET, see below) (Deniz et al., 1999; Ha et al., 1996) have been established quickly, paving the way for numerous applications in biology. Indeed, by attaching a fluorophore to a specific position of a POI, it becomes possible to monitor its structural dynamics, provided that the movement under study influences one of the aforementioned fluorescence properties. Note that single molecule fluorescence has been extensively used as well to monitor protein diffusion in living cells, evaluate protein oligomerization, and is at the basis of localization-based superresolution microscopies (Betzig et al., 2006; Hess et al., 2006; Rust et al., 2006). These application in the field of GPCR research have been reviewed extensively elsewhere (Tian et al., 2017), and are not subject of the present chapter that focuses on GPCR structural dynamics.

Single molecule Förster Resonance Energy Transfer (smFRET)

Förster Energy Transfer (FRET) is the spectroscopic mechanism by which the excitation energy form a fluorophore (the Donor (D)) is non-radiatively transferred to an absorbing molecule (the Acceptor (A)) (Clegg, 1995; Forster, 1948). Its efficiency depends on the spectral overlap between the two fluorophores and due to its nature (dipole-dipole interaction) to their relative orientation and their relative distance R given by the relation:

$$E = \frac{R_0^6}{R_0^6 + R^6}$$

, where R_0 the "Förster radius" is the characteristic distance for two fluorophores in a given environment, for which the probability of energy transfer is equal to 50% (E =

0.5). For pairs of fluorophores conventionally used in smFRET experiments, R_0 values are generally between 3 and 7 nm. This results in a range of measurable distances between about 2 nm and 11 nm (giving rise to an energy transfer probability between 5% and 95%), with accuracy as low as a few tenth of nm. Generally, conformational changes observed in smFRET experiments are reported as changes in apparent E values, which refer to changes in the inter-dye separation, without accurate quantification of the underlying distance. A precise distance determination is nevertheless possible, but it requires careful consideration of instrumental parameters as well as an experimental determination of R_0, defined as :

$R_0 = 978.\sqrt[6]{\Phi_D.\kappa^2.n^{-4}.J}$ (in nm)

This value depends on the quantum yield Φ_D of the donor in the absence of an acceptor, the refractive index n of the inter-fluorophore medium (which is estimated at n ~ 1.4 for biological macromolecules in aqueous solutions), the overlap integral J between the donor emission and acceptor absorption spectra (expressed in $M^{-1}.cm^3$), and the orientation factor κ^2. We refer the reader interested in accurate distance measurement to a recently published multi-laboratory benchmark study (Hellenkamp et al., 2017). Nevertheless, we would like to point out that although changes in transfer efficiency E reported in FRET experiments mainly result from variations in the inter-fluorophore distance, they can also arise from changes in the donor quantum yield Φ_D, as well as from changes in the relative orientation of the two fluorophores, which in turn affects κ^2, and thus R_0.

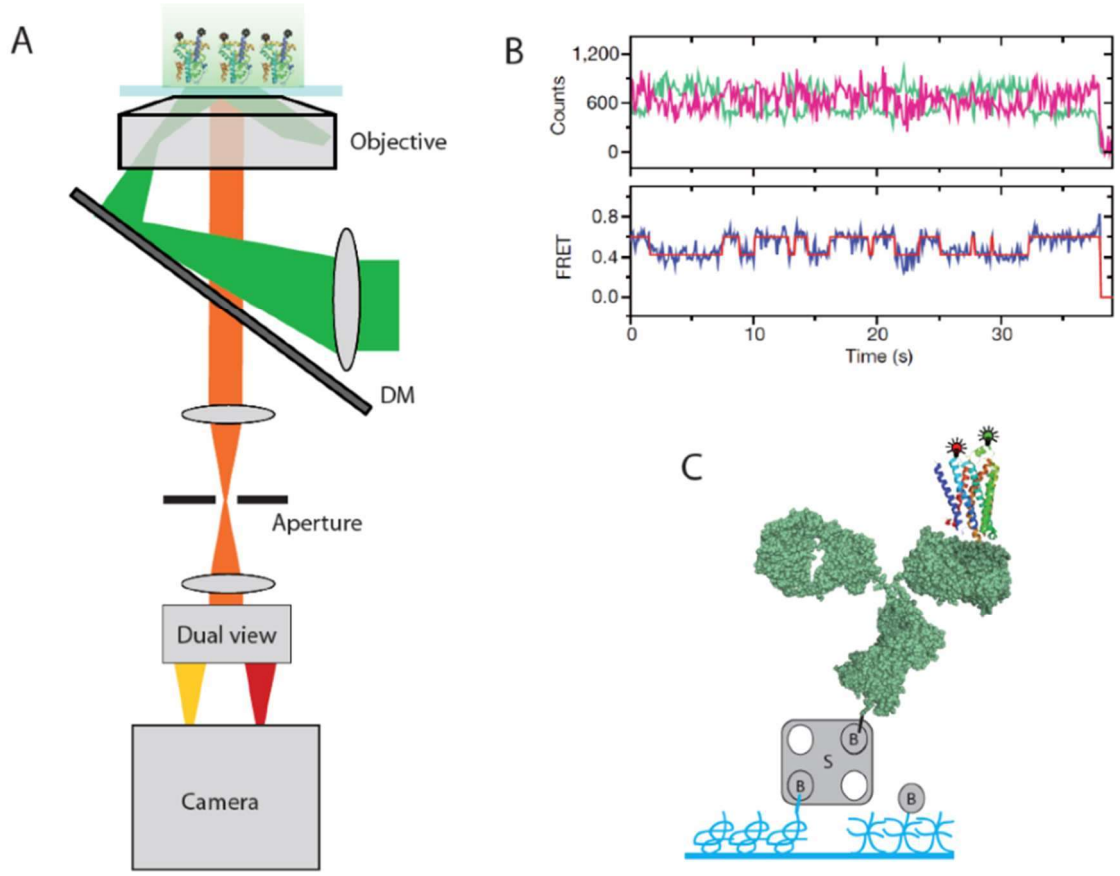

Figure 5: Single molecule observation by wide-field microscopy. (A) Typically an illumination based on total internal reflection (TIRF) is employed, coupled to a dual-view emission system for simultaneous monitoring the donor and acceptor signals in a FRET experiments. (B) This enables plotting for each single molecule the fluorescence intensities signal over extended periods of time, and calculating the FRET efficiency fluctuation. (C) Typical immuno-immobilization of a single molecule, where the glass surface is covalently modified by a polyethylene glycol (PEG) layer, mixed with a small fraction of biotin-PEG. A biotinylated antibody recognizing the POI (here, a GPCR, to scale) is immobilized via a biotin-streptavidin link.

Methods to detect single fluorescent molecules using a far-field microscope can be classified into two categories: wide-field microscopy, where a planar field of view (in which the molecules are generally attached) is illuminated and observed using a

camera, and confocal-type microscopy where point-illumination and detection are used.

In single molecule wide-field microscopy, an illumination scheme based on total internal reflexion is typically used (Figure 5A) (Axelrod, 2001). This permits to limit the excitation to a few hundreds of nanometers above the glass / medium interface, and thus strongly reduces the out-of-focus background. Until recently, EMCCD cameras were used for detection, but sCMOS have now been demonstrated to perform similarly well, for a reduced cost (Juette et al., 2016). For an smFRET experiment, the image has to be spectrally splitted, using a commercial or home-made dual view system (Kinosita et al., 1991) (Figure 5A). The wide field approach offers the advantage of visualizing hundreds of single molecules simultaneously, for durations up to minutes. For each molecule, changes in fluorescence properties as a function of time are obtained, forming a fluorescence intensity time trace (Figure 5B). Irreversible reactions can be monitored easily by flowing reagents during observation. However, the approach suffers from low time-resolution (typically 10-30 ms) that limits the observation to slow conformational changes, catalysis reactions, or molecular movements such as those of molecular motors on cytoskeleton filaments, or helicases or polymerases on nucleic acid templates. Moreover, measuring excited state lifetimes in the wide-field configuration is not a routine task, since camera that allow for time-resolved measurement at the nanosecond timescale generally lack the single molecule sensitivity. Finally, it requires the molecular complex of interest to be immobilized on the surface (Figure 5C) and therefore great care has to be taken to verify that the immobilization procedure does not perturb the conformational space of the protein. This is particularly important when the protein needs to be directly attached to a surface, as in the case of GPCR, where

immobilization has been traditionally achieved by direct binding of the protein to antibodies or nanobodies (Gregorio et al., 2017; Vafabakhsh et al., 2015) (Figure 5C). This problem is not present with nucleic-acid binding proteins for example, where the nucleic acid construct is itself immobilized (Ha et al., 2002; Margeat et al., 2006), or using strategies such as encapsulation of a soluble protein into liposomes (Cisse et al., 2007). In all cases, passivation of the surface with BSA or Polyethyleneglycol (PEG) is mandatory to minimize potential direct interactions of the POI with the surface.

In the case of point detection on diffusing molecules, a confocal-type observation geometry is used. A tightly focused laser beam defines a femtoliter-sized excitation volume, placed into an observation chamber (or a cell) containing the molecules of interest (Figure 6A). When the concentration of the labeled molecules is below ~1nM, the observation volume is empty most of the time, and each molecule diffusing through it will be detected as a "burst" of emitted photons (Nie et al., 1994) (Figure 6B,C). The detection configuration includes one to four detectors, generally avalanche photodiodes. One detector is enough for a simple intensity or excited-state lifetime measurement. Two spectrally distinct detectors are required to observe spectral emission variations, or for a multicolor experiment such as FRET. The additional measurement of fluorescence polarization requires a polarized excitation, and an additional separation of the emitted photons according to polarization. This 4-channel emission scheme is presented in Figure 6A and, when combined with a time-resolved detection allows for the measurement of all parameters of the fluorescence signal (an approach called multiparametric fluorescence detection (MFD) (Widengren et al., 2006)). More sophisticated geometries with up to 4 color detection for observation of multiple coordinated distance changes (Lee et al., 2010)

or multispot detection schemes to increase the throughput of the experiments and perform fast kinetic measurements (Ingargiola et al., 2017) have been described as well.

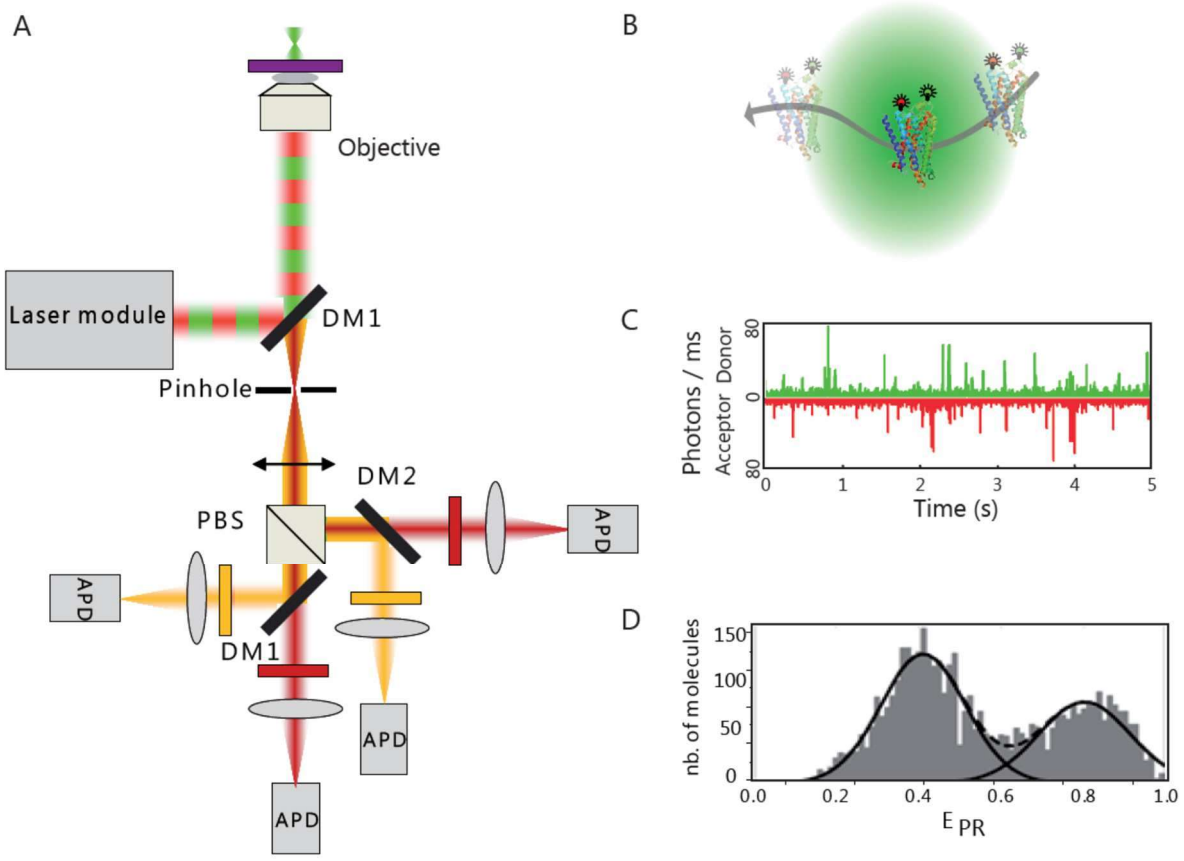

Figure 6: Single molecule observation on diffusing molecules. A pulsed interleaved / alternating laser excitation (PIE/ALEX) using two temporally separated excitation wavelength and up to four detectors (A) allows for a multiparameter fluorescence detection (MFD) on freely diffusing molecules passing through the observation volume (B). Donor and acceptor fluorescence signals are integrated for each single diffusing molecule with an excellent time resolution (C). Histograms representing the number of observed molecules as a function of a fluorescence parameter (here the apparent FRET efficiency E_{PR}) can then be plotted (D).

The typical analysis procedure for point-detection experiments involves the collection of all photons from each single molecule event, background subtraction, and calculation of the desired parameters including FRET efficiency, photon count rates, and when available excited state lifetimes and/or polarization. Typically they are

plotted on a 1D or 2D histogram displaying the number of molecules as a function of the individual parameter(s) (Figure 6D). We refer the reader to a recent benchmark study for a detailed presentation of the methods to calculate these parameters and extract inter-dye distance from smFRET measurements (Hellenkamp et al., 2017). In addition, for an smFRET experiment, it is recommended (Hellenkamp et al., 2017) to use a two-color alternating laser excitation scheme (PIE / ALEX) in order to account for fluorophore photophysical effects, to separate Donor-Acceptor species with low FRET efficiency from Donor-only molecules, and accurately calculate the correction factors needed for distance measurements (Hellenkamp et al., 2017; Kapanidis et al., 2004; Laurence et al., 2005; Lee et al., 2005; Müller et al., 2005).

The advantages of diffusion-based measurements are mainly two-fold (see also Table 1): first, it is not necessary to immobilize the molecule of interest, and thus its conformational dynamics remains unaffected. Second, the point detection using APDs permits an excellent time resolution, down to the microsecond (using continuous lasers and basic detection electronics (Deniz et al., 1999)) or even picosecond timescale (using pulsed lasers and Time-Correlated Single Photon Counting electronics (Widengren et al., 2006)). Thus, the timescales relevant for fast protein dynamics can be measured using this approach, as the various substates explored by the molecule of interest can be characterized. However, the photon flux for each single molecule is very low at these sub-ms timescales, precluding a direct observation of fluorescence signal changes as can be observed at longer timescales. Thus, most of the time, sophisticated data analysis procedures based on photon statistics have to be implemented such as Photon Distribution Analysis (PDA) (Antonik et al., 2006; Kalinin et al., 2008, 2007), Burst Variance Analysis (BVA) (Torella et al., 2011), correlation (FCS), cross correlation (FCCS) (Schwille et al.,

1997; Schwille and Haustein, 2009), filtered correlation spectroscopy (fFCS) (Felekyan et al., 2012), or species-integrated excited state lifetime measurements (Kalinin et al., 2010).

The main drawback of diffusion-based experiments as compared to those on immobilized molecules (see also Table 1) is that the upper limit of the timescale of events measurable is in the order of the observation time (ie the average time of the diffusion of the POI trough the confocal volume, that is typically in the millisecond range). Any conformational dynamics at slower timescales will result in the presence of multiple peaks that can be characterized in terms of fluorescence characteristics and relative abundance (which is directly related to their difference in free energy, see Figure 3). However, the kinetic parameters of the transition between these states (if any) can hardly be measured. It is also difficult with this method to look at irreversible reactions. Indeed, a typical measurement time to obtain relevant statistics on hundreds to thousands of single molecules is typically in the minutes to hours range. Thus, a time course experiment can only be measured if it is extremely slow. Nevertheless, using flow-based ultrafast mixers, very fast reactions can be characterized, as used in the field of protein folding for example (Hamadani and Weiss, 2008; Lipman, 2003; Wunderlich et al., 2013).

Table 1: Comparison of wide-field and confocal detection strategies.

	Wide field detection	Confocal detection
Immobilization	Necessary	Not necessary
Maximum time resolution	~ 10 ms	sub ns, typically µs
Observation time	limited by fluorophore photobleaching (~min)	limited by diffusion time (~ms)
Reversible reactions	Yes	Not easily
Microscope	TIRF / Camera	confocal (TCSPC if possible)

Combined strategies have been developed to overcome the limitations of each of these two approaches. For example, it is possible to perform a measurement using a confocal-based geometry on immobilized molecules, which provides the ability to monitor slow transitions with an excellent time resolution (Kim et al., 2002). Nevertheless, this geometry still requires protein immobilization, potentially perturbing its conformational dynamics. Therefore, immobilization strategies have been developed to localize proteins without perturbing them, such as encapsulation into liposomes (Boukobza et al., 2001) or more sophisticated approaches such as trapping into an anti-Brownian electrokinetic (ABEL) trap (Cohen and Moerner, 2006), introduced by the group of W.E. Moerner, notably to study β2 adrenergic receptors (β2AR) as described in more detail below (Bockenhauer et al., 2011).

Monitoring GPCR structural dynamics by single molecule fluorescence

Until now, SMF has been used to monitor two types of molecular movements in GPCR. Therefore, we will here first review the findings concerning the intracellular domain motions observed in class A GPCR, and try to relate them to general features of GPCR activation. Then, we will cover the observation made on the unique opening/closing and reorientation movements associated with the activation of class C GPCR extracellular domain.

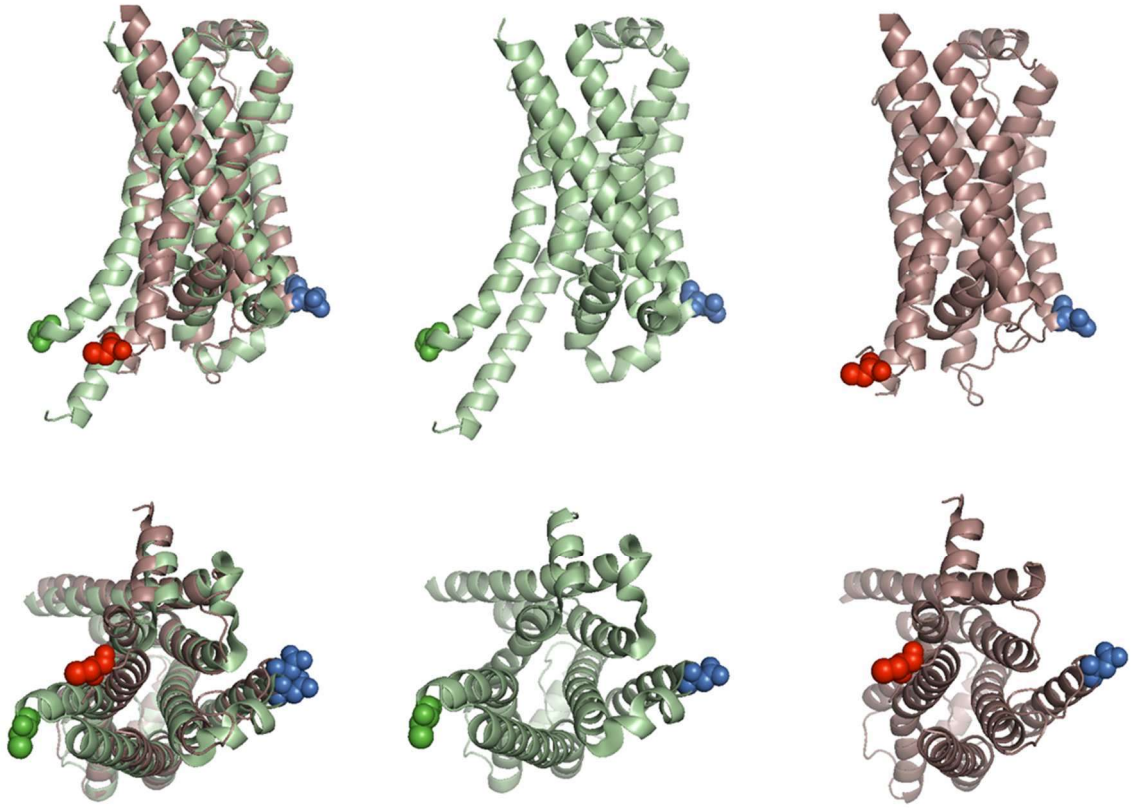

Figure 7: Cartoon representation of the β2AR receptor in the active (green, center, 3SN6) and inactive (red, right, 3RH1) conformations (left : overlay). Cys 265 that serves as reporter for TM6 movement during activation in several studies is represented by green and red balls. Cys148 (on TM4) that is used for dual color labeling in smFRET experiments is represented by blue balls.

The largest movements that seem to represent a common mechanism across different GPCRs have been found to occur in the intracellular region of the helix bundle, where conformational rearrangements including an outward movement of TM6 of up to 14 Å (as shown in the β2AR, see Figure 7) are necessary to accommodate the G protein and lead to full receptor activation (Rasmussen et al., 2011). An initial obstacle in the preparation of GPCRs suitable for single molecule studies was the preparation of labeled receptors in a functional and pure form. The first study showing fluorescence labeling of the β2AR took advantage of the high

sensitivity of the used fluorescent dye (IANBD) to its chemical environment (Gether et al., 1995). Slight changes in ensemble fluorescence intensity in response to agonists and antagonists were reported as resulting from receptor conformational changes. Nevertheless, the determined stoichiometry of fluorophore to receptor indicated labeling of more than a single cysteine residue. This problem was solved in a follow up study where fluorescein was coupled to the engineered receptor exclusively at C265 in ICL3 near the end of TM6 (Figure 7). Ensemble fluorescence lifetime measurements, that can report on the presence of receptor subpopulations, although not as accurately than single molecule measurements, revealed substantial changes in the environment of the dye (Ghanouni et al., 2001) in accordance with the rigid-body movement of TM6 described earlier for rhodopsin (Farrens et al., 1996). The data pointed at multiple distinct conformational states even at saturating agonist concentrations reflecting the inability of the agonist to fully activate the receptor and further underlining the high conformational flexibility of this prototypical class A GPCR. In the same year the first single molecule study of the β2AR was published, again indicating conformational heterogeneity of the receptor (Peleg et al., 2001). These experiments were performed on single diffusing molecules, and where therefore limited to short observation times of a few milliseconds per molecule. An important methodological implementation finally enabled monitoring structural dynamics at the single molecule level for the duration of several hundreds of milliseconds by trapping diffusing molecules in the field of view, through fast electrokinetic feedback to oppose Brownian motion (the so called ABEL trap) without perturbing its conformational freedom (Bockenhauer et al., 2011). In this way, the authors were able to provide evidence supporting the complex conformational landscape of the β2AR at the single molecule level and obtained information on the

influence of agonist binding on dwell times of conformational states, than spanned several orders of magnitude from milliseconds to seconds. The minor changes in conformation and interconversion dynamics observed upon addition of agonist pointed at the instability of the fully-activated conformational state, which was subsequently confirmed by structural and spectroscopic data that demonstrated the stabilizing effect of G protein (Manglik et al., 2015; Rasmussen et al., 2011; Rosenbaum et al., 2011). In contrast to the switch-like mechanism that leads to nearly full activation of rhodopsin (Altenbach et al., 2008), this general mechanism of allosteric stabilization essential for full activation seems to hold true also for other GPCRs and has in recent years facilitated to obtain active-like structures of a variety of different receptor including class A members such as the M2 muscarinic receptor (Kruse et al., 2013), the μ-opioid receptor (Huang et al., 2015), the A2a adenosine receptor (Carpenter et al., 2016; García-Nafría et al., 2018) and very recently the A1a receptor (Draper-Joyce et al., 2018) but also the calcitonin (Liang et al., 2017) and glucagon-like peptide-1 receptor (Zhang et al., 2017), which belong to the class B (for a recent review on active state structures of GPCRs see (Carpenter and Tate, 2017)).

In 2015 Lamichhane et al. reconstituted labeled β2AR in nanodiscs, tethered them to a surface and monitored the structural changes of the G protein binding domain in single molecules by TIRF microscopy taking advantage of the environmental sensitivity of Cy3 (Lamichhane et al., 2015), at a time resolution limited to 100ms. As seen before, the receptors where sampling between two conformations assigned to inactive and active states, with the inactive state being more highly populated in the absence of ligand. While the addition of agonist shifted the equilibrium towards the active, inverse agonist shifted it to the inactive

conformation. Examination of individual time trace trajectories revealed an enhanced frequency of activation events in the presence of agonist and a reduced frequency of sampling to the inactive state. Kinetic analysis of transitions between states identified two distinct rate constants for each of the transitions indicating that the populations of active as well as inactive receptors may each be composed of individual substates. Although, the authors provided convincing information on the relation between Cy3 fluorescence intensity fluctuations and conformational states of the receptor obtained by modeling the fluorescent label onto β2AR crystal structures (Cherezov et al., 2007; Rasmussen et al., 2011), a direct quantitative relation of fluorescence intensity fluctuations, arising from environmental changes, to distinct conformational rearrangements and states was not possible. This limitation has been overcome when Gregorio et al. presented the first smFRET study on a minimal cysteine variant of the β2AR. It was labeled with specifically optimized derivatives of Cy3B and Cy5 on engineered cysteines at 266 in TM6 and 148 in TM4 (Figure 7) to monitor the previously described displacement of TM6 in response to ligand-binding and G protein activation (Gregorio et al., 2017). The stimulation of surface-immobilized receptors with ligands of different efficacies correlated inversely with the FRET efficiency (Figure 8A) in accordance with an outward movement of TM6 increasing the average distance between the two fluorophores up to about 4Å in the presence of the full agonist adrenaline and in the absence of G protein. Inspection of individual time trajectories further revealed only rare fluctuations of an amplitude corresponding to the previously described relative displacement of TM6 by 14Å (Rasmussen et al., 2011). Fluorescence correlation analysis pointed at reversible TM6 movements faster than the time resolution of the imaging setup (>10 s^{-1}), with more rapid dynamics being observed for agonist-bound than antagonist-bound receptors.

Combined with simulations, the authors estimated TM6 deflections to lower FRET states at 2-10ms and explained the overall observed differences in comparison to previous studies (Lamichhane et al., 2015; Manglik et al., 2015) by differing experimental conditions and the nature of used probes.

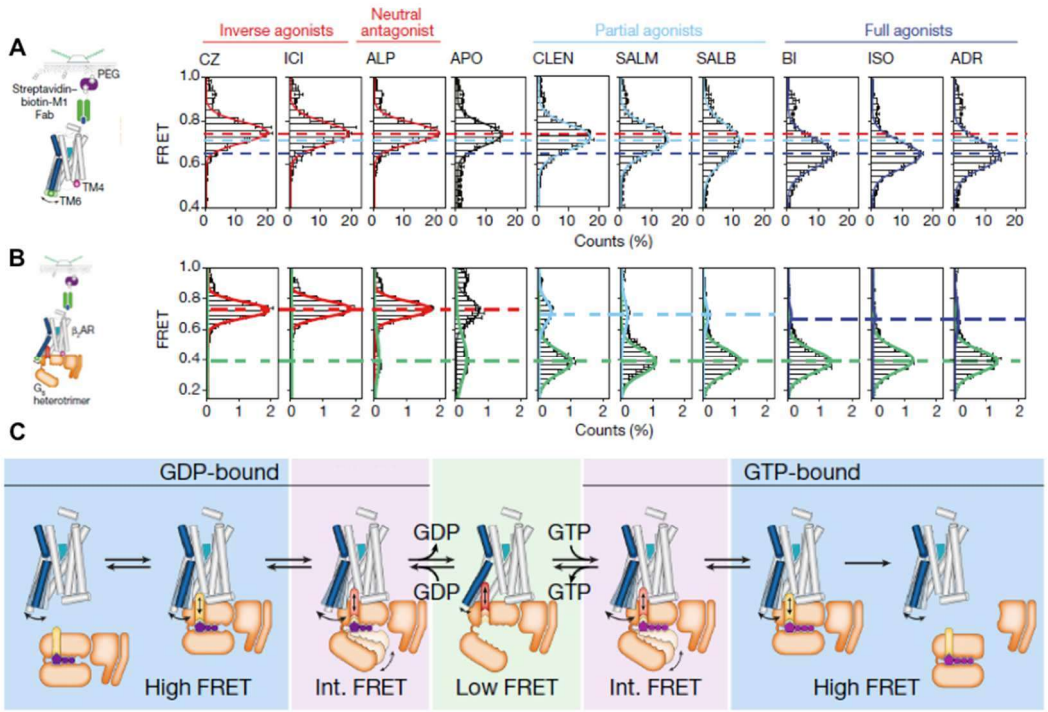

Figure 8: Influence of ligands and G protein on relative structural dynamics between TM4-TM6 in surface immobilized β2AR observed by TIRF microscopy. Ligands with different efficacy shift the conformational equilibrium according to their pharmacological effect (A). G protein is necessary to stabilize the fully active conformation represented by a low FRET state, which corresponds to a maximal distance between the two probes on the intracellular ends of TM4 and TM6 (B). Schematic model of TM6 conformation in relation to G protein binding, activation and nucleotide exchange (C). Figure adapted from (Gregorio et al., 2017).

Interestingly, the authors examined in that study the structural and kinetic changes triggered by the presence of the Gs heterotrimer. In the presence of agonists a distinct low-FRET state was observed (Figure 8B) with an approximate inter-dye distance of 55Å, likely corresponding to the outward movement of TM6. Time analysis led to the hypothesis that Gs coupling may be rate-limited by ligand-

dependent conformational rearrangements that occur within the inactive, high-FRET β2AR-Gs complex. Finally, the authors provided evidence for transient β2AR-Gs complexes in the presence of GDP and GTP and concluded that individual conformational changes related to ligands with varying efficacy regulate the rate at which the GDP-bound G protein-receptor complex is formed and also the efficiency of nucleotide exchange (Figure 8C).

This study represents a benchmark in the elucidation of GPCR conformational dynamics occurring in the intracellular part of the 7TMD and their relation to ligand efficacy and G protein activation but nevertheless, complementary studies at higher time resolution will be necessary to more precisely determine rates of interconversion between conformational states and potentially provide evidence for the presence of additional substates.

However, all these studies have been performed on the β2AR, and it will be necessary to evaluate to what extend these observation extends to other receptors. However, it is not always possible to engineer cysteine-less receptors, before adding a cystein residue at the required position for smFRET studies. Moreover, a complete study of conformational rearrangements throughout an entire receptor would require labeling at alternative positions and in combination with probes on the interacting G protein, to provide more information on concerted structural changes occurring in receptor and transducer. To achieve this and extend the studies to other GPCRs, alternative labeling strategies have to be developed, such as selective modification of cotranslationally incorporated non-canonical amino acids by genetic code expansion (Tian et al., 2017). A first step in that direction has been achieved using platelet-activating factor receptors (PAFRs), labeled on specifically incorporated azido-lyzines (AzK) and immobilized for smFRET experiments (Cao et al., 2018).

Although no dynamics were measured in that study, alternative configuration of TMD2 and TMD4 were observed, confirming observations from crystal structures showing that the PAFR adopts a distinct helical-bundle conformation with a respective outward movement of 13Å and 4Å when bound to the antagonist SR 27417 in comparison with the inverse agonist ABT-491.

Structural dynamics in the ECD of class C GPCRs

In contrast to most rhodopsin-like GPCRs including the β2AR and the PAFR many GPCRs from other classes contain a more or less extended N-terminal part that can function in ligand recognition, allosteric modulation, receptor dimerization and cooperativity as well as being a substrate for various posttranslational modifications including glycosylation and disulfide bridges (Lagerström and Schiöth, 2008). Among these types of receptors, only metabotropic glutamate receptors (mGluRs) have been observed by single molecule fluorescence to decipher their activation mechanism in real time. mGluRs are categorized as class C GPCRs, comprising a large extracellular domain (ECD) that has been shown to experience extensive conformational changes modulated by ligand binding (Scholler et al., 2017). G protein activation in response to their natural agonist glutamate requires mGluRs to be present in their native, dimeric form (El Moustaine et al., 2012), which has been shown to be partially mediated by an intermolecular disulfide bridge (Romano et al., 1996). Initial structural studies on isolated ECD dimers have revealed an antagonist-bound resting (R) state that experiences a relative reorientation by about 70° of the two ECDs upon agonist binding toward an active (A) state, that is accompanied with a closure of the Venus flytrap (VFT) bilobate domain (Figure 9) (Bessis et al., 2002; Kniazeff et al., 2004; Kunishima et al., 2000; Tsuchiya et al., 2002). Contradictory,

another study provided evidence that the ECD dimer can adopt conformations assigned to the active state in the presence of antagonist but also conformations assigned to the inactive state in the presence of agonist (Muto et al., 2007) (Figure 9).

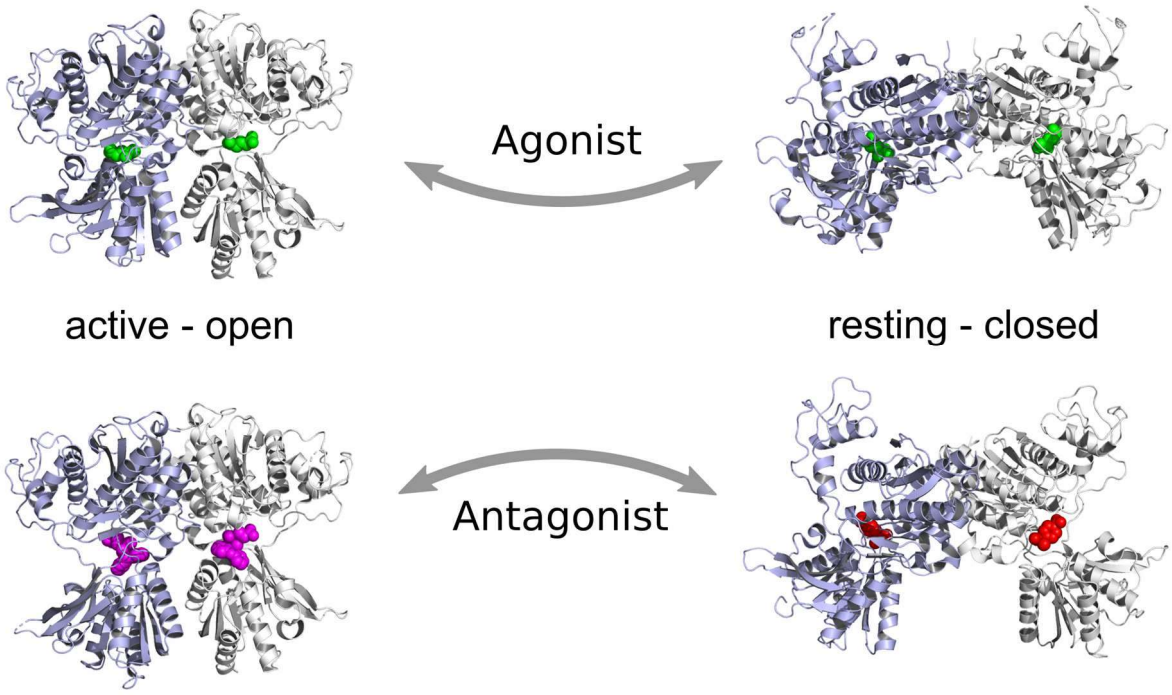

Figure 9: Implication of mGluR structural flexibility from contradictory crystal structures of isolated ECDs in the antagonist-bound (purple) active - open conformation (bottom left, 3KS9) and agonist-bound (green) resting - closed conformation (top right, 2E4U) as compared to the agonist-bound (green) active - open (top left, 1EWK) and antagonist-bound (red) resting - closed (bottom right, 1ISS).

An important step towards studying mGluR structural and dynamic features was the development of robust and highly specific labeling strategies including SNAP, HALO and CLIP tags N-terminally fused to the receptors. This facilitated sophisticated ensemble FRET studies on the dynamics of the extracellular domains in homo- but also heterodimers (Doumazane et al., 2013, 2011; El Moustaine et al., 2012; Møller et al., 2018), and confirmed the model of the ECD dimer reorientation upon agonist binding. For a more detailed review on ensemble FRET measurements of GPCR the reader is referred to the article of Banères and Rondard in this issue.

In a pioneering study, Olofsson et al. produced SNAP tag labeled dimers of isolated mGluR2 ECDs and monitored the transition dynamics from R to A states using single molecule FRET on freely diffusing molecules (Figure 10) (Olofsson et al., 2014). They demonstrate that the majority of the receptor ECDs oscillates between the resting and active states (characterized by a high FRET and a low FRET efficiency, respectively), in the absence and the presence of various ligands. This population of receptors appeared in their analysis as a distribution of molecules with a medium FRET (MF) efficiency (Figure 10a). This apparent MF value arises from the fact that the receptor ECD oscillates between the HF and LF states in the ~100μs timescale, ie much faster than the diffusion time of the receptor in the observation volume (Figure 10b, typically ~4ms), as demonstrated by several sophisticated correlation analysis procedures (2-color FCCS and fFCS). Since the FRET efficiency was calculated for the whole transit time of each single molecule in the volume, a MF value was obtained, that represented the time-averaged value of the two (HF and LF) states that the receptor ECDs explored during their diffusion.

In addition, a minor fraction of the ECDs were found to be “locked” in static LF and HF states, for time periods longer than the diffusion time (4ms). Whether these populations were able to transition to the fast dynamic state, represented by the MF population, was not determined in that study.

Interestingly, addition of ligands (either full agonists, partial agonists or antagonists) only affected the apparent FRET value of the MF population. Analysis of these data using dynamic photon distribution analysis (PDA) pointed at a model where the various ligands slightly influence the rate of resting to active state transitions rather than strongly stabilizing individual states. Even at saturating conditions of ligand, the receptor ECDs remained highly dynamic, pointing to a low activation energy barrier

and energy difference between the A and R states, which explained why it was able to crystalize in the R state in the presence of agonist, and in the A state when bound to an antagonist (Muto et al., 2007). In addition, this study demonstrated that partial agonists exert their activities, as far as the ECD is concerned, by loosely stabilizing the active state as compared to full agonists, instead of stabilizing a putative static, intermediate state between the R and A states.

These submillisecond conformational dynamics were observed for mGluR2, for mGluR4 and mGluR5 representing members of all mGluR subgroups, which gave rise to a general mechanism of activation conserved for all mGluR subtypes.

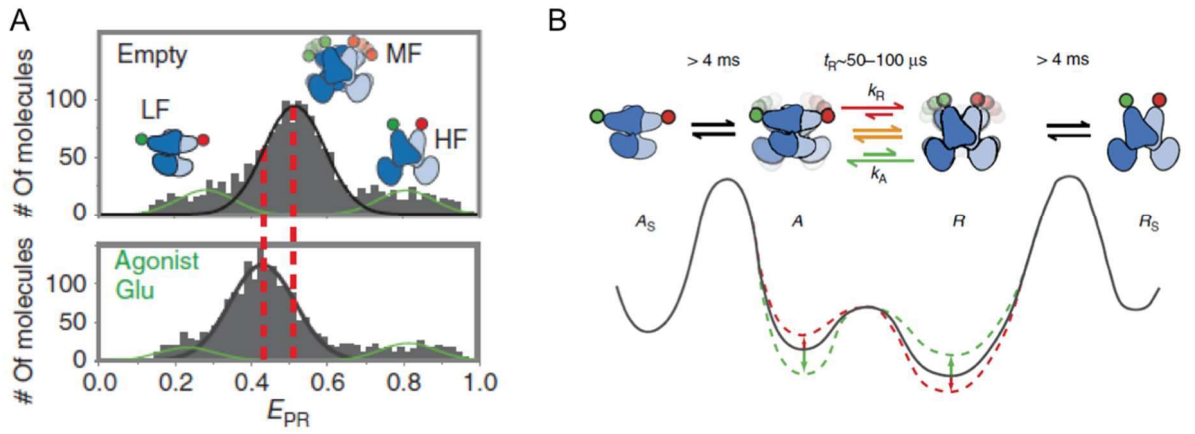

Figure 10: Submillisecond structural dynamics of isolated mGluR2 extracellular domain dimers observed in freely diffusing molecules by confocal microscopy. (A) In the absence of ligand (top) a predominant population of medium FRET intensity (MF) was observed located between low FRET/ active (LF) and high FRET/ resting states (HF). This population was shifted towards the LF in the presence of full agonist (bottom A). Analysis of transition rates revealed that the MF population consisted of two rapidly interchanging states (B). Figure adapted from (Olofsson et al., 2014).

In 2015 Vafabakhsh et al. published the first smFRET study on full-length mGluR2 and mGluR3, solubilized in detergent and C-terminally immunoimmobilized (Figure 11A) (Vafabakhsh et al., 2015). Due to the observation method (TIRF microscopy and wide field detection), these experiments were performed at a much slower time

resolution than the above-mentioned observations on diffusing ECD domains, and thus fast conformational dynamics, if present, were not resolved. The N-terminally CLIP and SNAP tag-labeled full-length dimers where found to populate three major states corresponding to high FRET/R, low FRET/A and a newly identified short-lived intermediate state (Figure 11B). Application of different orthosteric ligands including full and partial agonists (Figure 11C) led to the conclusion that ligand efficacy is determined by occupancy of the low FRET/A state rather than by promoting individual conformations corresponding to varying degrees of VFT domain closure, which is in accordance with the model of Olofsson et al. on the ECD where ligands modulate the rates of transitions between states (Olofsson et al., 2014). Based on dwell times of the high and low FRET states that were found to be in the range of tens of milliseconds up to seconds under the given conditions (Figure 11D), the authors proposed that the ligand binding domain (LBD) in the resting and active states may be stabilized by the TMD of the full-length receptors leading to longer occupancies than seen on isolated ECD dimers. Finally, they demonstrated kinetic differences between mGluR2 and mGluR3, with the latter exhibiting a more stable A state and an apparent sensitivity to physiological Ca^{2+} concentrations in agreement with its basal activity observed in the absence of ligands. It is however likely that this latter observation arises from the effect of chloride ions (present through the use of $CaCl_2$), that have more recently been shown to stabilize the glutamate-induced active state of mGluR3, by pharmacological, modeling and single molecule FRET experiments (Tora et al., 2018).

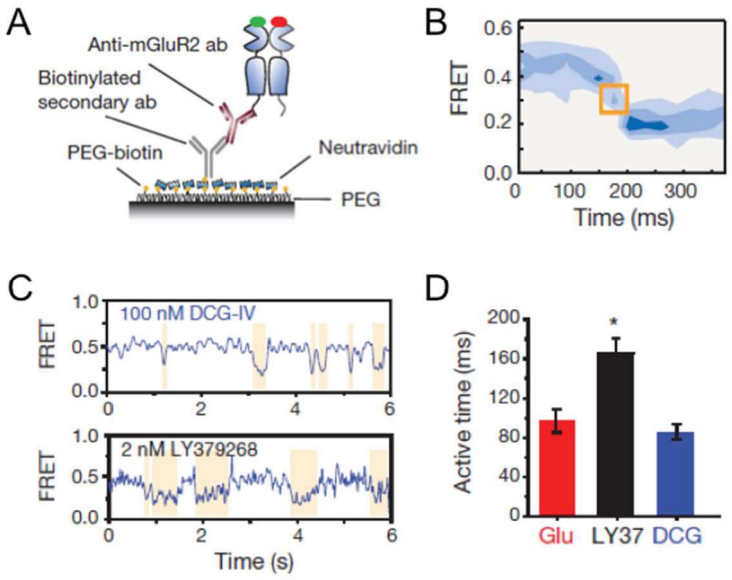

Figure 11: Slow conformational dynamics on surface immobilized full-length mGluR2 observed by TIRF microscopy. Observation of immunoimmobilized mGluR2 dimers (A) revealed a novel intermediate FRET population (B) and analysis of time trajectories from applications of ligands with different efficacies (C) implicated that ligand efficacy is determined by occupancy of the low FRET state. Dwell time analysis (D) further revealed much longer residence times in the active / low FRET state that seen before on isolated ECDs by Olofsson et al. Figure was adapted from (Vafabakhsh et al., 2015).

In the following, this study was extended to investigate the cooperativity of homomeric and heteromeric mGluRs. (Levitz et al., 2016). Single-molecule subunit counting in cells was completed to differential receptor activation using photo-switchable tethered agonists, as well as single molecule FRET on surface immobilized full length receptors, labeled as previously at their N-terminus via protein tags. Mutational analysis correlated with conformational state occupancies and led to the conclusions that hydrophobic contacts at the level of the LBD interface may stabilize the R conformation of the ECD to prevent its basal activity, while at the same time limiting glutamate sensitivity, whereas the disulfide bridge (C121) rather stabilizes the A state. Finally, the authors proposed a model of cooperative receptor

activation where ligand induced closure of one LBD leads to an allosteric shift in the dynamic equilibrium of the unliganded subunit, which in the case of mGluR2/mGluR3 heterodimers may determine efficacy.

Conclusion and Outlook

It is striking that the vast majority of published single molecule fluorescence studies on GPCR structural dynamics have so far been limited to only two receptors, the β_2AR and the mGluR. However, these two receptors can be considered prototypical models for the class-A and class-C GPCRs and have therefore received major attention from pharmacologist, structural biologists, and biophysists.

The β_2AR can now be expressed and purified in relatively large quantities and appears reasonably stable even in detergents, thanks to more than 2 decades of intense research focus (Lefkowitz, 2013), which explains its use in many structural and biophysical studies. SMF studies on this receptor performed in the last 20 years have increased in sophistication and level of details but they have all focused on the observation of the movement of the internal tip of TM6 relative to the core of the receptor 7TM or particularly to TM4. All studies point to a model, where the receptor in its apo or ligand bound states explores various conformations at the submillisecond timescale. Ligands push this conformational ensemble toward a set of configurations according to their pharmacology. Nevertheless the interaction with the G-protein appears necessary for a strong stabilization of the fully activated state, for longer times, in accordance with observations inferred from X-ray crystallography (Rasmussen et al., 2011) or NMR (Nygaard et al., 2013).

Interestingly, similar submillisecond dynamics have been observed in the case of the extracellular domain of mGluRs, where ligand binding only pushed the

conformational ensemble toward configurations prone to activation or inhibition of receptor activity (Olofsson et al., 2014). The active conformation is probably stabilized for extended periods of time upon agonist binding in the context of the full length receptor (Levitz et al., 2016; Vafabakhsh et al., 2015). However, it should be noted that the conformational changes at the level of the 7TM domain of mGluR have not been explored yet at the single molecule level. The activation of this receptor includes conformational changes occurring throughout all its domains (ECD, CRD, 7TM), including a relative reorientation of them within the dimer (Doumazane et al., 2011; Koehl et al., 2019; Olofsson et al., 2014; Xue et al., 2015). A detailed understanding of the structural dynamics of this receptor, the coordinated conformational changes within and between its domains, and the allosteric effects of ligands or other effectors, will require a careful site-specific labeling of the various modules and the investigation of their movements with high time and spatial resolution.

Altogether, the SMF observations on these two receptors point to a similar model of high conformational flexibility within the receptor, even in the presence of ligands. The molecular basis of partial agonism has been unveiled, showing that these pharmacophore partial activity stems from their low efficiency to modify the conformational ensemble, rather than their ability to stabilize alternative, partially active states.

SMF experiments should now be extended towards new directions for a better understanding of the complete activation mechanism of GPCRs.

First, it would be useful and necessary to verify that the findings obtained on these model receptors can be generalized to others, including class-B GPCR.

Then, the structural dynamics profile of the receptors needs now to be studied in the context of their interactions with other partners (such as in the case of β2AR / G protein complex (Gregorio et al., 2017)). This is particularly relevant to better understand the molecular basis of biaised agonism, as it could be proposed that the pharmacological profile of these ligands stems from their ability to populate various states for different time periods, leading to differential interaction kinetics of the receptors with their partners. Similarly, some receptors have been shown to dimerize or multimerize under the influence of ligands (Gurevich and Gurevich, 2018; Kasai and Kusumi, 2014; Møller et al., 2018), and how these protein/protein interactions influence the structural dynamics of the receptor and its interactions with its effectors remains to be explored.

In addition, minimally invasive labeling strategies like the use of selectively reactive non-canonical amino acids enable the attachment of SMF-suitable fluorophores in a bioorthogonal manner at practically any desired position within the receptors and its ligands (Tian et al., 2017, 2014). This open the way to individually fine-tune the experimental conditions to achieve a maximal sensitivity for conformational changes to be probed throughout the entire receptors and increase the accuracy of the acquired data with regard to both the functional integrity of receptors but also the interpretability of movement-induced photophysical phenomena (Milles et al., 2012; Quast et al., 2019; Sadoine et al., 2017). In this way the relative conformational changes between individual receptor domains and their chronology during activation may be monitored.

Finally, the influence of the native membrane environment including its lipid but also protein composition and surrounding matrix may significantly alter not only the amplitude but also the rates of conformational transitions in an allosteric fashion.

Therefore it is very likely that in the future, substantial additional information on GPCR structure / dynamics / function relationships will be gathered from smFRET investigations in nanodiscs (Nath et al., 2010), proteoliposomes (Börsch et al., 2002; Kim et al., 2015; Wang et al., 2015) and eventually on live cells (Calebiro and Koszegi, 2019; Sungkaworn et al., 2017).

Acknowledgements

Our research is supported by a grant from the Agence Nationale pour la Recherche (ANR-12-BSV2-0015). Our laboratory belongs to the France-BioImaging national infrastructure supported by the French National Research Agency (ANR-10-INBS-04, " Investments for the future"). The graphical abstract figure has been prepared using the FPS software from C. Seidel Lab (U. of Dusseldorf) (Kalinin et al. Nat. Methods 9, 1218-1225 (2012)).

References

Alhadeff, R., Vorobyov, I., Yoon, H.W., Warshel, A., 2018. Exploring the free-energy landscape of GPCR activation. Proc. Natl. Acad. Sci. 115, 10327–10332. https://doi.org/10.1073/pnas.1810316115

Altenbach, C., Kusnetzow, A.K., Ernst, O.P., Hofmann, K.P., Hubbell, W.L., 2008. High-resolution distance mapping in rhodopsin reveals the pattern of helix movement due to activation. Proc. Natl. Acad. Sci. 105, 7439–7444. https://doi.org/10.1073/PNAS.0802515105

Antonik, M., Felekyan, S., Gaiduk, A., Seidel, C.A.M., 2006. Separating structural heterogeneities

from stochastic variations in fluorescence resonance energy transfer distributions via photon distribution analysis. J. Phys. Chem. B 110, 6970–8. https://doi.org/10.1021/jp057257+

Ashkin, A., Dziedzic, J.M., Yamane, T., 1987. Optical trapping and manipulation of single cells using infrared laser beams. Nature 330, 769–771. https://doi.org/10.1038/330769a0

Axelrod, D., 2001. Selective imaging of surface fluorescence with very high aperture microscope objectives. J Biomed Opt 6, 6–13.

Bessis, A., Rondard, P., Gaven, F., Brabet, I., Triballeau, N., Pre, L., Acher, F., Pin, J., 2002. Closure of the Venus flytrap module of mGlu8 receptor and the activation process : Insights from mutations converting antagonists into agonists 99, 11097–11102.

Betzig, E., Patterson, G.H., Sougrat, R., Lindwasser, O.W., Olenych, S., Bonifacino, J.S., Davidson, M.W., Lippincott-Schwartz, J., Hess, H.F., 2006. Imaging intracellular fluorescent proteins at nanometer resolution. Science (80-.). 313, 1642–1645. https://doi.org/10.1126/science.1127344

Bockenhauer, S., Fürstenberg, A., Yao, X.J., Kobilka, B.K., Moerner, W.E., 2011. Conformational Dynamics of Single G Protein-Coupled Receptors in Solution. J. Phys. Chem. B 115, 13328–13338. https://doi.org/10.1021/jp204843r

Börsch, M., Diez, M., Zimmermann, B., Reuter, R., Gräber, P., 2002. Stepwise rotation of the gamma-subunit of EF0F1-ATP synthase observed by intramolecular single-molecule fluorescence resonance energy transfer. FEBS Lett. 527, 147–152. https://doi.org/10.1016/S0014-5793(02)03198-8

Boukobza, E., Sonnenfeld, A., Haran, G., 2001. Immobilization in surface-tethered lipid vesicles as a new tool for single biomolecule spectroscopy. J. Phys. Chem. B 105, 12165–12170. https://doi.org/10.1021/jp012016x

Calebiro, D., Koszegi, Z., 2019. The subcellular dynamics of GPCR signaling. Mol. Cell. Endocrinol. 483, 24–30. https://doi.org/10.1016/j.mce.2018.12.020

Cao, C., Tan, Q., Xu, C., He, L., Yang, L., Zhou, Ye, Zhou, Yiwei, Qiao, A., Lu, M., Yi, C., Han, G.W., Wang, X., Li, X., Yang, H., Rao, Z., Jiang, H., Zhao, Y., Liu, J., Stevens, R.C., Zhao, Q., Zhang, X.C., Wu, B., 2018. Structural basis for signal recognition and transduction by platelet-activating-factor receptor. Nat. Struct. Mol. Biol. 1–8. https://doi.org/10.1038/s41594-018-0068-y

Carpenter, B., Nehmé, R., Warne, T., Leslie, A.G.W., Tate, C.G., 2016. Structure of the adenosine A2A receptor bound to an engineered G protein. Nature 536, 104–107.

https://doi.org/10.1038/nature18966

Carpenter, B., Tate, C.G., 2017. Active state structures of G protein-coupled receptors highlight the similarities and differences in the G protein and arrestin coupling interfaces. Curr. Opin. Struct. Biol. 45, 124–132. https://doi.org/10.1016/J.SBI.2017.04.010

Casiraghi, M., Point, E., Pozza, A., Moncoq, K., Banères, J.L., Catoire, L.J., 2019. NMR analysis of GPCR conformational landscapes and dynamics. Mol. Cell. Endocrinol. 484, 69–77. https://doi.org/10.1016/j.mce.2018.12.019

Cherezov, V., Rosenbaum, D.M., Hanson, M.A., Rasmussen, S.G.F., Thian, F.S., Kobilka, T.S., Choi, H., Kuhn, P., Weis, W.I., Kobilka, B.K., Stevens, R.C., 2007. High-Resolution Crystal Structure of an Engineered Human b 2 -Adrenergic. Science (80-.). 318, 1258–1266. https://doi.org/10.1126/science.1150577

Cisse, I., Okumus, B., Joo, C., Ha, T., 2007. Fueling protein DNA interactions inside porous nanocontainers. Proc. Natl. Acad. Sci. U. S. A. 104, 12646–12650. https://doi.org/10.1073/pnas.0610673104

Clegg, R.M., 1995. Fluorescence resonance energy transfer. Curr. Opin. Biotechnol. 6, 103–110. https://doi.org/10.1016/0958-1669(95)80016-6

Cohen, A.E., Moerner, W.E., 2006. Suppressing Brownian motion of individual biomolecules in solution. Proc. Natl. Acad. Sci. 103, 4362–4365. https://doi.org/10.1073/pnas.0509976103

Deniz, a a, Dahan, M., Grunwell, J.R., Ha, T., Faulhaber, A.E., Chemla, D.S., Weiss, S., Schultz, P.G., 1999. Single-pair fluorescence resonance energy transfer on freely diffusing molecules: observation of Förster distance dependence and subpopulations. Proc. Natl. Acad. Sci. U. S. A. 96, 3670–5.

Doumazane, E., Scholler, P., Fabre, L., Zwier, J.M., Trinquet, E., Pin, J.-P., Rondard, P., 2013. Illuminating the activation mechanisms and allosteric properties of metabotropic glutamate receptors. Proc. Natl. Acad. Sci. U. S. A. 110, E1416-25. https://doi.org/10.1073/pnas.1215615110

Doumazane, E., Scholler, P., Zwier, J.M., Trinquet, E., Rondard, P., Pin, J.-P., 2011. A new approach to analyze cell surface protein complexes reveals specific heterodimeric metabotropic glutamate receptors. FASEB J. 25, 66–77. https://doi.org/10.1096/fj.10-163147

Draper-Joyce, C.J., Khoshouei, M., Thal, D.M., Liang, Y.-L., Nguyen, A.T.N., Furness, S.G.B.,

Venugopal, H., Baltos, J.-A., Plitzko, J.M., Danev, R., Baumeister, W., May, L.T., Wootten, D., Sexton, P.M., Glukhova, A., Christopoulos, A., 2018. Structure of the adenosine-bound human adenosine A1 receptor–Gi complex. Nature 558, 559–563. https://doi.org/10.1038/s41586-018-0236-6

El Moustaine, D., Granier, S., Doumazane, E., Scholler, P., Rahmeh, R., Bron, P., Mouillac, B., Banères, J.-L., Rondard, P., Pin, J.-P., 2012. Distinct roles of metabotropic glutamate receptor dimerization in agonist activation and G-protein coupling. Proc. Natl. Acad. Sci. U. S. A. 109, 16342–7. https://doi.org/10.1073/pnas.1205838109

Engel, A., Gaub, H.E., Müller, D.J., 1999. Atomic force microscopy: A forceful way with single molecules. Curr. Biol. https://doi.org/10.1016/S0960-9822(99)80081-5

Erlandson, S.C., McMahon, C., Kruse, A.C., 2018. Structural Basis for G Protein–Coupled Receptor Signaling. Annu. Rev. Biophys. 47, annurev-biophys-070317-032931. https://doi.org/10.1146/annurev-biophys-070317-032931

Farrens, D.L., Altenbach, C., Yang, K., Hubbell, W.L., Khorana, H.G., 1996. Requirement of rigid-body motion of transmembrane helices for light activation of rhodopsin. Science 274, 768–70. https://doi.org/10.1126/SCIENCE.274.5288.768

Felekyan, S., Kalinin, S., Sanabria, H., Valeri, A., Seidel, C. a. M., 2012. Filtered FCS: species auto- and cross-correlation functions highlight binding and dynamics in biomolecules. ChemPhysChem 13, 1036–1053. https://doi.org/10.1002/cphc.201100897

Felekyan, S., Sanabria, H., Kalinin, S., Kühnemuth, R., Seidel, C.A.M., 2013. Analyzing förster resonance energy transfer with fluctuation algorithms. Methods Enzymol. 519, 39–85. https://doi.org/10.1016/B978-0-12-405539-1.00002-6

Forster, T., 1948. Zwichenmolekulare Energiewanderung und Fluoreszenz. Ann. Phys. 6, 166–175. https://doi.org/10.1007/BF00585226

García-Nafría, J., Lee, Y., Bai, X., Carpenter, B., Tate, C.G., 2018. Cryo-EM structure of the adenosine A2A receptor coupled to an engineered heterotrimeric G protein. Elife 7. https://doi.org/10.7554/eLife.35946

Gether, U., Lin, S., Kobilka, B.K., 1995. Fluorescent labeling of purified beta 2 adrenergic receptor. Evidence for ligand-specific conformational changes. J. Biol. Chem. 270, 28268–28275. https://doi.org/10.1074/jbc.270.47.28268

Ghanouni, P., Gryczynski, Z., Steenhuis, J.J., Lee, T.W., Farrens, D.L., Lakowicz, J.R., Kobilka, B.K., 2001. Functionally different agonists induce distinct conformations in the G protein coupling domain of the beta 2 adrenergic receptor. J. Biol. Chem. 276, 24433–6. https://doi.org/10.1074/jbc.C100162200

Gopich, I. V, Szabo, A., 2010. FRET efficiency distributions of multistate single molecules. J. Phys. Chem. B 114, 15221–6. https://doi.org/10.1021/jp105359z

Gregorio, G.G., Masureel, M., Hilger, D., Terry, D.S., Juette, M., Zhao, H., Zhou, Z., Perez-Aguilar, J.M., Hauge, M., Mathiasen, S., Javitch, J.A., Weinstein, H., Kobilka, B.K., Blanchard, S.C., 2017. Single-molecule analysis of ligand efficacy in β2AR-G-protein activation. Nature 547, 68–73. https://doi.org/10.1038/nature22354

Gurevich, V. V., Gurevich, E. V., 2018. GPCRs and Signal Transducers: Interaction Stoichiometry. Trends Pharmacol. Sci. 39, 672–684. https://doi.org/10.1016/J.TIPS.2018.04.002

Ha, T., Enderle, T., Ogletree, D.F., Chemla, D.S., Selvin, P.R., Weiss, S., 1996. Probing the interaction between two single molecules: fluorescence resonance energy transfer between a single donor and a single acceptor. Proc Natl Acad Sci U S A 93, 6264–6268.

Ha, T., Glass, J., Enderle, T., Chemla, D.S., Weiss, S., 1998. Hindered rotation diffusion and rotational jumps of single molecules. Phys. Rev. Lett. 80, 2093–2096.

Ha, T., Rasnik, I., Cheng, W., Babcock, H.P., Gauss, G.H., Lohman, T.M., Chu, S., 2002. Initiation and re-initiation of DNA unwinding by the Escherichia coli Rep helicase. Nature 419, 638–41.

Hamadani, K.M., Weiss, S., 2008. Nonequilibrium single molecule protein folding in a coaxial mixer. Biophys. J. 95, 352–65. https://doi.org/10.1529/biophysj.107.127431

Hellenkamp, B., Schmid, S., Doroshenko, O., Opanasyuk, O., Kühnemuth, R., Adariani, S.R., Barth, A., Birkedal, V., Bowen, M.E., Chen, H., Cordes, T., Eilert, T., Fijen, C., Götz, M., Gouridis, G., Gratton, E., Ha, T., Hanke, C.A., Hartmann, A., Hendrix, J., Hildebrandt, L.L., Hohlbein, J., Hübner, C.G., Kallis, E., Kapanidis, A.N., Kim, J.-Y., Krainer, G., Lamb, D.C., Lee, N.K., Lemke, E.A., Levesque, B., Levitus, M., McCann, J.J., Naredi-Rainer, N., Nettels, D., Ngo, T., Qiu, R., Röcker, C., Sanabria, H., Schlierf, M., Schuler, B., Seidel, H., Streit, L., Tinnefeld, P., Tyagi, S., Vandenberk, N., Weninger, K.R., Wünsch, B., Yanez-Orozco, I.S., Michaelis, J., Seidel, C.A.M., Craggs, T.D., Hugel, T., 2017. Precision and accuracy of single-molecule FRET measurements - a worldwide benchmark study 1–27.

Henzler-Wildman, K., Kern, D., 2007. Dynamic personalities of proteins. Nature 450, 964–972. https://doi.org/10.1038/nature06522

Hess, S.T., Girirajan, T.P., Mason, M.D., 2006. Ultra-high resolution imaging by fluorescence photoactivation localization microscopy. Biophys J 91, 4258–4272.

Hollingsworth, S.A., Dror, R.O., 2018. Review Molecular Dynamics Simulation for All. Neuron 99, 1129–1143. https://doi.org/10.1016/j.neuron.2018.08.011

Huang, W., Manglik, A., Venkatakrishnan, A.J., Laeremans, T., Feinberg, E.N., Sanborn, A.L., Kato, H.E., Livingston, K.E., Thorsen, T.S., Kling, R.C., Granier, S., Gmeiner, P., Husbands, S.M., Traynor, J.R., Weis, W.I., Steyaert, J., Dror, R.O., Kobilka, B.K., 2015. Structural insights into μ-opioid receptor activation. Nature 524, 315–321. https://doi.org/10.1038/nature14886

Ingargiola, A., Lerner, E., Chung, S., Panzeri, F., Gulinatti, A., Rech, I., Ghioni, M., Weiss, S., Michalet, X., 2017. Multispot single-molecule FRET: Highthroughput analysis of freely diffusing molecules. PLoS One 12. https://doi.org/10.1371/journal.pone.0175766

Juette, M.F., Terry, D.S., Wasserman, M.R., Altman, R.B., Zhou, Z., Zhao, H., Blanchard, S.C., 2016. Single-Molecule Imaging of Non-Equilibrium Molecular Ensembles on the Millisecond Timescale. Nat. Methods 1–7. https://doi.org/10.1038/nmeth.3769

Kalinin, S., Felekyan, S., Antonik, M., Seidel, C.A.M., 2007. Probability distribution analysis of single-molecule fluorescence anisotropy and resonance energy transfer. J. Phys. Chem. B 111, 10253–62. https://doi.org/10.1021/jp072293p

Kalinin, S., Felekyan, S., Valeri, A., Seidel, C.A.M., 2008. Characterizing multiple molecular States in single-molecule multiparameter fluorescence detection by probability distribution analysis. J. Phys. Chem. B 112, 8361–74. https://doi.org/10.1021/jp711942q

Kalinin, S., Valeri, A., Antonik, M., Felekyan, S., Seidel, C.A.M., 2010. Detection of structural dynamics by FRET: a photon distribution and fluorescence lifetime analysis of systems with multiple states. J. Phys. Chem. B 114, 7983–95. https://doi.org/10.1021/jp102156t

Kapanidis, A., Lee, N.-K., Laurence, T., Doose, S., Margeat, E., Weiss, S., 2004. Fluorescence-aided molecule sorting. Analysis of structure and interactions by alternating laser excitation of single molecules. Proc. Nat. Acad. Sci. USA 101, 8936–8941.

Kasai, R.S., Kusumi, A., 2014. Single-molecule imaging revealed dynamic GPCR dimerization. Curr. Opin. Cell Biol. 27, 78–86. https://doi.org/10.1016/j.ceb.2013.11.008

Kim, H.D., Nienhaus, G.U., Ha, T., Orr, J.W., Williamson, J.R., Chu, S., 2002. Mg2+-dependent conformational change of RNA studied by fluorescence correlation and FRET on immobilized single molecules. Proc Natl Acad Sci U S A 99, 4284–4289.

Kim, J.-Y., Kim, C., Lee, N.K., 2015. Real-time submillisecond single-molecule FRET dynamics of freely diffusing molecules with liposome tethering. Nat. Comm. 6, 6992. https://doi.org/10.1038/ncomms7992

Kinosita, K., Itoh, H., Ishiwata, S., Hirano, K., Nishizaka, T., Hayakawa, T., 1991. Dual-view microscopy with a single camera - real-time imaging of molecular orientations and calcium. J. Cell Biol. 115, 67–73.

Kniazeff, J., Bessis, A.-S., Maurel, D., Ansanay, H., Prézeau, L., Pin, J.-P., 2004. Closed state of both binding domains of homodimeric mGlu receptors is required for full activity. Nat. Struct. Mol. Biol. 11, 706–713. https://doi.org/10.1038/nsmb794

Koehl, A., Hu, H., Feng, D., Sun, B., Zhang, Y., Robertson, M.J., Chu, M., Kobilka, T.S., Laeremans, T., Steyaert, J., Tarrasch, J., Dutta, S., Fonseca, R., Weis, W.I., Mathiesen, J.M., Skiniotis, G., Kobilka, B.K., 2019. Structural insights into the activation of metabotropic glutamate receptors. Nature 566, 79–84. https://doi.org/10.1038/s41586-019-0881-4

Kruse, A.C., Ring, A.M., Manglik, A., Hu, J., Hu, K., Eitel, K., Hübner, H., Pardon, E., Valant, C., Sexton, P.M., Christopoulos, A., Felder, C.C., Gmeiner, P., Steyaert, J., Weis, W.I., Garcia, K.C., Wess, J., Kobilka, B.K., 2013. Activation and allosteric modulation of a muscarinic acetylcholine receptor. Nature 504, 101–106. https://doi.org/10.1038/nature12735

Kunishima, N., Shimada, Y., Tsuji, Y., Sato, T., Yamamoto, M., Kumasaka, T., Nakanishi, S., Jingami, H., Morikawa, K., 2000. Structural basis of glutamate recognition by a dimeric metabotropic glutamate receptor. Nature 407, 971–977. https://doi.org/10.1038/35039564

Lagerström, M.C., Schiöth, H.B., 2008. Structural diversity of G protein-coupled receptors and significance for drug discovery. Nat. Rev. Drug Discov. 7, 339.

Lakowicz, J.R., 2006. Principles of fluorescence spectroscopy. Springer International Publishing.

Lamichhane, R., Liu, J.J., Pljevaljcic, G., White, K.L., van der Schans, E., Katritch, V., Stevens, R.C., Wüthrich, K., Millar, D.P., 2015. Single-molecule view of basal activity and activation mechanisms of the G protein-coupled receptor β 2 AR. Proc. Natl. Acad. Sci. 112, 14254–14259. https://doi.org/10.1073/pnas.1519626112

Latorraca, N.R., Venkatakrishnan, A.J., Dror, R.O., 2017. GPCR Dynamics: Structures in Motion. Chem. Rev. 117, 139–155. https://doi.org/10.1021/acs.chemrev.6b00177

Laurence, T. a, Kong, X., Jäger, M., Weiss, S., 2005. Probing structural heterogeneities and fluctuations of nucleic acids and denatured proteins. Proc. Natl. Acad. Sci. U. S. A. 102, 17348–53. https://doi.org/10.1073/pnas.0508584102

Laurence, T.A., Kapanidis, A.N., Kong, X., Chemla, D.S., Weiss, S., 2004. Photon Arrival-Time Interval Distribution (PAID): A Novel Tool for Analyzing Molecular Interactions. J. Phys. Chem. B 108, 3051–3067.

Lee, J., Lee, S., Ragunathan, K., Joo, C., Ha, T., Hohng, S., 2010. Single-molecule Four-color FRET. Angew. Chem. Int. Ed. Engl. 49, 9922–25. https://doi.org/10.1158/0008-5472.CAN-10-4002.BONE

Lee, N.K., Kapanidis, A.N., Wang, Y., Michalet, X., Mukhopadhyay, J., Ebright, R.H., Weiss, S., 2005. Accurate FRET Measurements within Single Diffusing Biomolecules using Alternating-laser Excitation. Biophys. J. 88, 2939–2943.

Lefkowitz, R.J., 2013. A brief history of G-protein coupled receptors (Nobel Lecture). Angew. Chemie - Int. Ed. 52, 6366–6378. https://doi.org/10.1002/anie.201301924

Levitz, J., Habrian, C., Bharill, S., Fu, Z., Vafabakhsh, R., Isacoff, E.Y., 2016. Mechanism of Assembly and Cooperativity of Homomeric and Heteromeric Metabotropic Glutamate Receptors. Neuron 92, 143–159. https://doi.org/10.1016/j.neuron.2016.08.036

Liang, Y.-L., Khoshouei, M., Radjainia, M., Zhang, Y., Glukhova, A., Tarrasch, J., Thal, D.M., Furness, S.G.B., Christopoulos, G., Coudrat, T., Danev, R., Baumeister, W., Miller, L.J., Christopoulos, A., Kobilka, B.K., Wootten, D., Skiniotis, G., Sexton, P.M., 2017. Phase-plate cryo-EM structure of a class B GPCR–G-protein complex. Nature 546, 118–123. https://doi.org/10.1038/nature22327

Lipman, E.A., 2003. Single-Molecule Measurement of Protein Folding Kinetics. Science (80-.). 301, 1233–1235. https://doi.org/10.1126/science.1085399

Macklin, J.J., Trautman, J.K., Harris, T.D., Brus, L.E., 1996. Imaging and Time-Resolved Spectroscopy of Single Molecules at an Interface. Science (80-.). 272, 255–258.

Manglik, A., Kim, T.H., Masureel, M., Altenbach, C., Yang, Z., Hilger, D., Lerch, M.T., Kobilka, T.S., Thian, F.S., Hubbell, W.L., Prosser, R.S., Kobilka, B.K., 2015. Structural insights into the dynamic process of β<inf>2</inf>-adrenergic receptor signaling. Cell 161, 1101–1111.

https://doi.org/10.1016/j.cell.2015.04.043

Margeat, E., Kapanidis, A.N., Tinnefeld, P., Wang, Y., Mukhopadhyay, J., Ebright, R.H., Weiss, S., 2006. Direct observation of abortive initiation and promoter escape within single immobilized transcription complexes. Biophys. J. 90, 1419–1431.

McKinney, S.A., Joo, C., Ha, T., 2006. Analysis of single-molecule FRET trajectories using hidden Markov modeling. Biophys. J. 91, 1941–1951. https://doi.org/10.1529/biophysj.106.082487

Mehta, A.D., Rief, M., Spudich, J.A., Smith, D.A., Simmons, R.M., 1999. Single-Molecule Biomechanics with Optical Methods 283, 1689–1696.

Milles, S., Tyagi, S., Banterle, N., Koehler, C., VanDelinder, V., Plass, T., Neal, A.P., Lemke, E.A., 2012. Click Strategies for Single-Molecule Protein Fluorescence. J. Am. Chem. Soc. 134, 5187–5195. https://doi.org/10.1021/ja210587q

Møller, T.C., Hottin, J., Clerté, C., Zwier, J.M., Durroux, T., Rondard, P., Prézeau, L., Royer, C.A., Pin, J.P., Margeat, E., Kniazeff, J., 2018. Oligomerization of a G protein-coupled receptor in neurons controlled by its structural dynamics. Sci. Rep. 8, 1–15. https://doi.org/10.1038/s41598-018-28682-6

Müller, B.K., Zaychikov, E., Bräuchle, C., Lamb, D.C., Muller, B.K., Brauchle, C., 2005. Pulsed interleaved excitation. Biophys. J. 89, 3508–22. https://doi.org/10.1529/biophysj.105.064766

Muller, R., Zander, C., Sauer, M., Deimel, M., Ko, D.S., Siebert, S., Arden-Jacob, J., Deltau, G., Marx, N., Drexhage, K., Wolfrum, J., 1996. Time-resolved identification of single molecules in solution with a pulsed semiconductor diode laser. Chem. Phys. Lett. 262, 716–22.

Muto, T., Tsuchiya, D., Morikawa, K., Jingami, H., 2007. Structures of the extracellular regions of the group II/III metabotropic glutamate receptors. Proc. Natl. Acad. Sci. U. S. A. 104, 3759–64. https://doi.org/10.1073/pnas.0611577104

Nath, A., Trexler, A.J., Koo, P., Miranker, A.D., Atkins, W.M., Rhoades, E., 2010. Single-molecule fluorescence spectroscopy using phospholipid bilayer nanodiscs. Methods Enzymol. 472, 89–117. https://doi.org/10.1016/S0076-6879(10)72014-0

Nie, S., Chiu, D., Zare, R.N., 1994. Probing Individual Molecules with Confocal Fluorescence Microscopy. Science (80-.). 266, 1018–1021.

Nygaard, R., Zou, Y., Dror, R.O., Mildorf, T.J., Arlow, D.H., Manglik, A., Pan, A.C., Liu, C.W., Fung, J.J., Bokoch, M.P., Thian, F.S., Kobilka, T.S., Shaw, D.E., Mueller, L., Prosser, R.S., Kobilka,

B.K., 2013. The dynamic process of β(2)-adrenergic receptor activation. Cell 152, 532–42. https://doi.org/10.1016/j.cell.2013.01.008

Olofsson, L., Felekyan, S., Doumazane, E., Scholler, P., Fabre, L., Zwier, J.M., Rondard, P., Seidel, C.A.M., Pin, J.-P., Margeat, E., 2014. Fine tuning of sub-millisecond conformational dynamics controls metabotropic glutamate receptors agonist efficacy. Nat. Commun. 5, 5206.

Peleg, G., Ghanouni, P., Kobilka, B.K., Zare, R.N., 2001. Single-molecule spectroscopy of the beta(2) adrenergic receptor: observation of conformational substates in a membrane protein. Proc Natl Acad Sci U S A 98, 8469–8474.

Quast, R.B., Fatemi, F., Kranendonk, M., Margeat, E., Truan, G., 2019. Accurate Determination of Human CPR Conformational Equilibrium by smFRET Using Dual Orthogonal Noncanonical Amino Acid Labeling. ChemBioChem 20, 659–666. https://doi.org/10.1002/cbic.201800607

Rasmussen, S.G.F., DeVree, B.T., Zou, Y., Kruse, A.C., Chung, K.Y., Kobilka, T.S., Thian, F.S., Chae, P.S., Pardon, E., Calinski, D., Mathiesen, J.M., Shah, S.T.A., Lyons, J.A., Caffrey, M., Gellman, S.H., Steyaert, J., Skiniotis, G., Weis, W.I., Sunahara, R.K., Kobilka, B.K., 2011. Crystal structure of the β2 adrenergic receptor–Gs protein complex. Nature 477, 549–555. https://doi.org/10.1038/nature10361

Romano, C., Yang, W.L., O'Malley, K.L., 1996. Metabotropic glutamate receptor 5 is a disulfide-linked dimer. J. Biol. Chem. 271, 28612–6. https://doi.org/10.1074/JBC.271.45.28612

Rosenbaum, D.M., Zhang, C., Lyons, J.A., Holl, R., Aragao, D., Arlow, D.H., Rasmussen, S.G.F., Choi, H.-J., DeVree, B.T., Sunahara, R.K., Chae, P.S., Gellman, S.H., Dror, R.O., Shaw, D.E., Weis, W.I., Caffrey, M., Gmeiner, P., Kobilka, B.K., 2011. Structure and function of an irreversible agonist-β2 adrenoceptor complex. Nature 469, 236–240. https://doi.org/10.1038/nature09665

Rust, M.J., Bates, M., Zhuang, X., 2006. Sub-diffraction-limit imaging by stochastic optical reconstruction microscopy (STORM). Nat. Methods 5–7. https://doi.org/10.1038/NMETH929

Sackmann, B., Sakmann, B., 1992. Elementary steps in synaptic transmission revealed by currents through single ion channels. Neuron 8, 613–629.

Sadoine, M., Cerminara, M., Kempf, N., Gerrits, M., Fitter, J., Katranidis, A., 2017. Selective Double-Labeling of Cell-Free Synthesized Proteins for More Accurate smFRET Studies. Anal. Chem. 89, 11278–11285. https://doi.org/10.1021/acs.analchem.7b01639

Schmidt, T., Schütz, G.J., Baumgartner, W., Gruber, H.J., Schindler, H., 1996. Imaging of single molecule diffusion. Proc. Natl. Acad. Sci. 93, 2926–2929. https://doi.org/10.1073/pnas.93.7.2926

Scholler, P., Moreno-Delgado, D., Lecat-Guillet, N., Doumazane, E., Monnier, C., Charrier-Savournin, F., Fabre, L., Chouvet, C., Soldevila, S., Lamarque, L., Donsimoni, G., Roux, T., Zwier, J.M., Trinquet, E., Rondard, P., Pin, J.-P., 2017. HTS-compatible FRET-based conformational sensors clarify membrane receptor activation. Nat. Chem. Biol. 13, 372–380. https://doi.org/10.1038/nchembio.2286

Schwille, P., Haustein, E., 2009. Fluorescence correlation spectroscopy An introduction to its concepts and applications. Spectroscopy 1–33.

Schwille, P., Meyer-Almes, F.J., Rigler, R., 1997. Dual-color fluorescence cross-correlation spectroscopy for multicomponent diffusional analysis in solution. Biophys. J. 72, 1878–86.

Smith, J.S., Lefkowitz, R.J., Rajagopal, S., 2018. Biased signalling: from simple switches to allosteric microprocessors. Nat. Rev. Drug Discov. 17, 243–260. https://doi.org/10.1038/nrd.2017.229

Soper, S.A., Keller, R.A., Seitzinger, N.K., Davis, L.M., Brooks Shera, E., 1990. Detection of single fluorescent molecules. Chem. Phys. Lett. 174, 553–557. https://doi.org/10.1016/0009-2614(90)85485-u

Strick, T.R., Allemand, J., Bensimon, D., Bensimon, A., Croquette, V., 1996. The Elasticity of a Single Supercoiled DNA Molecule 271, 1835–1838.

Sungkaworn, T., Jobin, M.L., Burnecki, K., Weron, A., Lohse, M.J., Calebiro, D., 2017. Single-molecule imaging reveals receptor-G protein interactions at cell surface hot spots. Nature 550, 543–547. https://doi.org/10.1038/nature24264

Thal, D.M., Glukhova, A., Sexton, P.M., Christopoulos, A., 2018. Structural insights into G-protein-coupled receptor allostery. Nature 559, 45–53. https://doi.org/10.1038/s41586-018-0259-z

Tian, H., Furstenberg, A., Huber, T., 2017. Labeling and single-molecule methods to monitor G proteincoupled receptor dynamics. Chem. Rev. 117, 186–245. https://doi.org/10.1021/acs.chemrev.6b00084

Tian, H., Naganathan, S., Kazmi, M.A., Schwartz, T.W., Sakmar, T.P., Huber, T., 2014. Bioorthogonal Fluorescent Labeling of Functional G-Protein-Coupled Receptors. ChemBioChem 15, 1820–1829. https://doi.org/10.1002/cbic.201402193

Tora, A.S., Rovira, X., Cao, A.-M., Cabayé, A., Olofsson, L., Malhaire, F., Scholler, P., Baik, H., Van

Eeckhaut, A., Smolders, I., Rondard, P., Margeat, E., Acher, F., Pin, J.-P., Goudet, C., 2018. Chloride ions stabilize the glutamate-induced active state of the metabotropic glutamate receptor 3. Neuropharmacology 140, 275–286. https://doi.org/10.1016/J.NEUROPHARM.2018.08.011

Torella, J.P., Holden, S.J., Santoso, Y., Hohlbein, J., Kapanidis, A.N., 2011. Identifying molecular dynamics in single-molecule FRET experiments with burst variance analysis. Biophys. J. 100, 1568–77. https://doi.org/10.1016/j.bpj.2011.01.066

Tsuchiya, D., Kunishima, N., Kamiya, N., Jingami, H., Morikawa, K., 2002. Structural views of the ligand-binding cores of a metabotropic glutamate receptor complexed with an antagonist and both glutamate and Gd3+. Proc. Natl. Acad. Sci. U. S. A. 99, 2660–5. https://doi.org/10.1073/pnas.052708599

Vafabakhsh, R., Levitz, J., Isacoff, E.Y., 2015. Conformational dynamics of a class C G-protein-coupled receptor. Nature 524, 497–501. https://doi.org/10.1038/nature14679

Wacker, D., Stevens, R.C., Roth, B.L., 2017. How Ligands Illuminate GPCR Molecular Pharmacology. Cell 170, 414–427. https://doi.org/10.1016/j.cell.2017.07.009

Wang, S., Vafabakhsh, R., Borschel, W.F., Ha, T., Nichols, C.G., 2015. Structural dynamics of potassium-channel gating revealed by single-molecule FRET. Nat. Struct. Mol. Biol. 23, 1–7. https://doi.org/10.1038/nsmb.3138

Weis, W.I., Kobilka, B.K., 2018. The Molecular Basis of G Protein-Coupled Receptor Activation. Annu. Rev. Biochem. https://doi.org/10.1146/annurev-biochem-060614-033910

Weiss, S., 1999. Fluorescence spectroscopy of single biomolecules. Science (80-.). 283, 1676–83.

Widengren, J., Kudryavtsev, V., Antonik, M., Berger, S., Gerken, M., Seidel, C.A.M., 2006. Single-molecule detection and identification of multiple species by multiparameter fluorescence detection. Anal.Chem. 78, 2039–2050. https://doi.org/10.1021/ac0522759

Wingler, L.M., Elgeti, M., Hilger, D., Latorraca, N.R., Lerch, M.T., Staus, D.P., Dror, R.O., Kobilka, B.K., Hubbell, W.L., Lefkowitz, R.J., 2019. Angiotensin Analogs with Divergent Bias Stabilize Distinct Receptor Conformations. Cell 176, 468-478.e11. https://doi.org/10.1016/j.cell.2018.12.005

Wunderlich, B., Nettels, D., Benke, S., Clark, J., Weidner, S., Hofmann, H., Pfeil, S.H., Schuler, B., 2013. Microfluidic mixer designed for performing single-molecule kinetics with confocal detection on timescales from milliseconds to minutes. Nat. Protoc. 8, 1459–1474.

https://doi.org/10.1038/nprot.2013.082

Xue, L., Rovira, X., Scholler, P., Zhao, H., Liu, J., Pin, J.-P., Rondard, P., 2015. Major ligand-induced rearrangement of the heptahelical domain interface in a GPCR dimer. Nat. Chem. Biol. 11, 134–140. https://doi.org/10.1038/nchembio.1711

Zhang, Y., Sun, B., Feng, D., Hu, H., Chu, M., Qu, Q., Tarrasch, J.T., Li, S., Sun Kobilka, T., Kobilka, B.K., Skiniotis, G., 2017. Cryo-EM structure of the activated GLP-1 receptor in complex with a G protein. Nature 546, 248–253. https://doi.org/10.1038/nature22394